DERIVATION OF FUNCTIONAL SPINAL CORD NEURONS FROM INDUCED PLURIPOTENT STEM CELLS (IPSCS) VIA NEUROMESODERMAL PROGENITORS (NMPS)

by
Ezgi Bulut

Submitted to Gradutae School of Natural Applied Sciences
In Partial Fulfillment of the Requirements
For the degree of Master of Science in
Biotechnology

Yeditepe University
2022

DERIVATION OF FUNCTIONAL SPINAL CORD NEURONS FROM INDUCED PLURIPOTENT STEM CELLS (IPSCS) VIA NEUROMESODERMAL PROGENITORS (NMPS)

APPROVED BY:

Assoc. Prof. Dr. Ayşegül Doğan ……
(Thesis Supervisor)
(Yeditepe University)

Prof. Dr. Fikrettin Şahin ……
(Yeditepe University)

Prof. Dr. Ahmet Arman ……
(Marmara University)

DATE OF APPROVAL: ..../..../2022

I hereby declare that this thesis is my own work and that all information in this thesis has been obtained and presented in accordance with academic rules and ethical conduct. I have fully cited and referenced all material and results as required by these rules and conduct, and this thesis study does not contain any plagiarism. If any material used in the thesis requires copyright, the necessary permissions have been obtained. No material from this thesis has been used for the award of another degree.

I accept all kinds of legal liability that may arise in case contrary to these situations.

Name, Last name Ezgi Bulut

Signature …..…….……..

ACKNOWLEDGEMENTS

I would like to express my deep and sincere gratitude to my thesis supervisor Assoc. Prof. Dr Ayşegül Doğan for her amazing knowledge and profound guidance and for giving me an opportunity to work with her project in her laboratory.

I would like to express my special thanks to my laboratory members, PhD. Taha Bartu Hayal, PhD candidate Selinay Şenkal and PhD candidate Hatice Burcu Şişli with their unlimited support and unconditional help during my master thesis. Additionally, I would like to thank PhD. Pınar Akkuş Süt for helping during microscopy.

Finally and most importantly, I would like to thank my family, thank to my mother Aysu Bulut, my father Özcan Bulut and my brother Ali Cem Bulut for their endless love and understanding.

ABSTRACT

DERIVATION OF FUNCTIONAL SPINAL CORD NEURONS FROM INDUCED PLURIPOTENT STEM CELLS (IPSCS) VIA NEUROMESODERMAL PROGENITORS (NMPS)

Induced pluripotent stem cells (iPSCs) are generated by reprogramming of cells somatic cells in laboratory conditions. Although iPSCs are promising sources of cellular therapy, there are some ethical and physiological problems in using iPSCs in therapy. Therefore, the identification of safe progenitor cells derived from pluripotent stem cells is critical to control the differentiation capacity of pluripotent cells. Neuromesodermal progenitor (NMP) cells are found in primitive streak region as a bipotent cell population, which can give rise to the paraxial mesoderm and spinal cord during development. Motor neuron diseases (MND) are fatal and progressive diseases that result in the destruction of motor neurons. In motor neuron diseases, motor neurons lose their ability to control muscle cells causing walking, breathing, and speaking problems. Spinal muscular atrophy (SMA), Amyotrophic lateral sclerosis (ALS) and spinal cord injury are the most common motor neuron diseases that have not effective treatments. The pharmacological treatments only provide to extend life span and get strengthen life conditions. In this thesis, NMPs were derived from iPSCs, differentiated into spinal cord neurons and characterized. Functional neurons were characterized in vitro by identification of cellular and molecular mechanisms.

ÖZET

NÖROMEZODERMAL KÖK HÜCRELER ARACILIĞIYLA UYARILMIŞ PLURİPOTENT KÖK HÜCRELERDEN (UPK) FONKSİYONEL OMURİLİK NÖRONLARININ TÜRETİLMESİ

Uyarılmış pluripotent kök hücreler (UPKC) somatik hücrelerin laboratuvar koşullarında yeniden programlanmasıyla üretilir. UPKC'ler umut verici hücresel terapi kaynakları olmasına rağmen, UPKC'lerin terapide kullanılmasında bazı etik ve fizyolojik sorunlar vardır. Bu nedenle, pluripotent kök hücrelerden türetilen güvenli progenitör hücrelerin tanımlanması, pluripotent hücrelerin farklılaşma kapasitesini kontrol etmek için kritik öneme sahiptir. Nöromezodermal progenitörler (NMP'ler), paraksiyal mezoderm ve omuriliğe farklılaşabilen, ilkel çizgi bölgesinde bulunanmultipotent hücre popülasyonudur. Motor nöron hastalıkları (MNH), motor nöronların yıkımıyla sonuçlanan ölümcül ve ilerleyici hastalıklardır. Motor nöron hastalıklarında motor nöronlar, kas hücrelerini kontrol etme yeteneklerini kaybederek yürüme, nefes alma ve konuşma sorunlarına neden olurlar. Spinal müsküler atrofi (SMA), Amyotrofik lateral skleroz (ALS) ve omurilik yaralanması etkili tedavileri olmayan en sık görülen motor nöron hastalıklarıdır. Farmakolojik tedaviler sadece yaşam süresini uzatmayı ve yaşam koşullarını güçlendirmeyi sağlar. Bu tezde, NMP'ler UPKC'lerden türetilip, omurilik nöronlarına farklılaştırılmış ve karakterize edilmiştir. Fonksiyonel nöronlar, hücresel ve moleküler mekanizmaların tanımlanmasıyla in vitro olarak karakterize edildi.

TABLE OF CONTENTS

LIST OF FIGURES

LIST OF TABLES

LIST OF SYMBOLLS/ABBREVATIONS

°C	Degree centigrade
mL	Mililiter
ng	Nanogram
nM	Nanomolar
µL	Microliter
µm	Micrometer
µM	Micromolar

ALS	Amytrophic lateral sclerosis
AR	Apelin receptor
BSA	Bovine serum albumin
BM-MSCs	Bone marrow mesenchymal stem cells
c-Myc	Bird myelocytomatosis virus oncogene cellular homologue
CD	Cluster of differentiation
cDNA	Complementary deoxyribonucleic acid
CE	Caudal epiblast
CNS	Central nervous system
CLE	Caudal lateral epiblast
DMEM	Dulbecco's modified eagle's medium
DMSO	Dimethyl sulfoxide
ES	Embryonic stem
ESCs	Embryonic stem cells
FBS	Fetal bovine serum
FGF	Fibroblast growth factor
FGF-2	Fibroblast growth factor 2
qPCR	Real time polymerase chain reaction
HOX	Homebox genes
ICC	Immunocytochemistry
Isl-1	Islet-1
Isl-2	Islet-2
iPSCs	Induced pluripotent stem cells

Klf4	Kruppel-like factor 4
KRT14	Keratin 14
LC MS	Liquid chromotography mass spectroscopy
LIF	Leukemia inhibitory factor
MACF1	Microtubule actin crosslinking factor 1
mESCs	mouse embryonic stem cells
MMLV	Moloney murine leukemia virus
MND	Motor neuron diseases
MRCL3	Myosin regulatory light chain
MSCs	Mesencymal stem cells
Neun	Neuronal nuclei
NF	Neural filamet
NMP	Neuromesodermal progenitors
NMJ	Neuromuscular junctions
Oct4	Octamer-binding transcription factor 4
Oct4/3	Octamer-binding transcription factor 4/3
PAX3	Paired bax protein 3
PAX6	Paired bax protein 3
PBS	Phosphate buffer saline
PDGF	Platelet-derived growth factor
PFA	Paraformaldehyde
PS	Primitive streak
PSA	Penicillin, streptomycin and amphotericin B
PSCs	Pluripotent stem cells
RA	Retinoic acid
SEM	Scanning electron microscopy
Shh	Sonic hedgehog.
SC	Spinal cord
SCI	Spinal cord injury
SMA	Spinal muscular atrophy
SNAP23	Synaptosomal-associated protein 23
Sox-2	Sex determining region Y-box 2
SSEA1	Stage specific embryonic antigen

T/Bra	Brachyury
TEM	Transmission electron microscopy
TGF	Transforming growth factor
TH	Tyrosine hydroxylase
VEGF	Vascular endothelial growth factor
Wnt	Wingless/Integrated

1. INTRODUCTION

1.1. STEM CELLS

Stem cells are undifferentiated cells that have ability of self-renewal and differentiation into other cell types [1]. During the division of stem cells, one cell differentiates into a specific cell type which have a different function and phenotype, and the other one remains as a stem cell as indicated in Figure 1.1. Cytokines, transcription factors, cell-to-cell and cell-to-cell matrices all promote stem cell differentiation into specialized cells [2]. They are found in both embryos and adult [1].

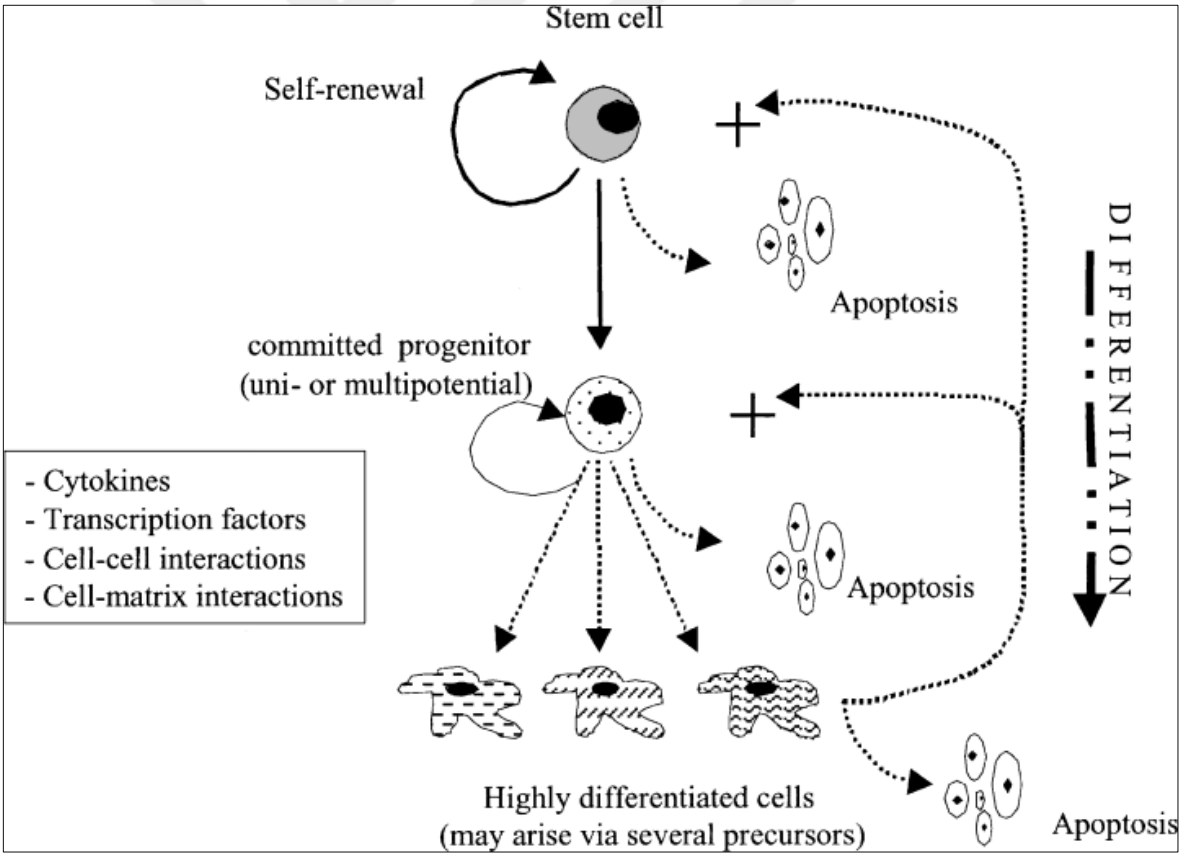

Figure 1.1. Overview of Stem cell fate [2]

The potency of stem cells is number and range of phenotype. During developmental process, differentiation capacity reduces [3]. For instance, unipotent stem cells cannot differentiate as pluripotent stem cells. Therefore, stem cells are divided into four groups based on their

potency. First one is totipotent stem cells have the ability to divide and differentiate into whole organism. Another one is pluripotent stem cells differentiate into all cells except for extraembryonic tissues such as placenta. Although multipotent stem cells have restricted differentiation capacity as pluripotent stem cells, they can develop many progenitor cells. Last one is unipotent stem cells can differentiate into one type of cells [4].

Adult stem cells, embryonic stem cells, and induced pluripotent stem cells are the three types of stem cells based on their origin. Adult stem cells are also known as somatic stem cells that are found in the specific niches [5]. The adult stem cells are important to maintain the integrity of skin, bone and blood [3]. The hematopoietic stem cells (HSCs) and mesenchymal stem cells (MSCs) are the part of adult stem cells. Mesenchymal stem cells are present in many tissues, and they differentiate into bone, cartilage and adipogenic cells. Hematopoietic stem cells differentiate into blood cells. Skin stem cells form a protective layer of skin [6].

The cues that influence stem cell specialization can be classified as internal or external. External signals involve physical contact between cells or chemical secretion by surrounding tissues, whereas internal signals are regulated by genes. [5]. The other function of stem cells is participating internal repair system of the body [7]. While an organism is alive, formation of new cells and replenishment are unlimited. However, stem cell activity varies according to organ location. For example, the division of stem cells in bone marrow is continual. [5]. On the other hand, in pancreas, stem cells divide only special conditions [8].

Stem cells are used to drug development and toxicity test. They allow faster drug development [9]. Additionally, stem cells have important role of regenerative medicine to cell therapy. Adult stem cells of bone marrow have been used for cancer treatments for many years [10]. For instance, HSCs have been used to treatment of leukaemia and lymphoma with bone marrow transplantation since 1960s [11]. Recently, ability of MSCs give rise bone and cartilage, they are used to medicate degenerative changes in the joint, reconstructing bone and cartilage, using in plastic surgery, cardiovascular diseases, and repair of damaged musculoskeletal tissues [12].

1.2. PLURIPOTENT STEM CELL

Pluripotent stem cells (PSCs) have the ability to differentiate into three primary germ layers: endoderm, ectoderm and mesoderm. Endoderm is the inner layer of three germ layer. It can differentiate gastrointestinal tracts and lung. Wnt and activin A drives to endoderm fate [13]. Also, endoderm layer expressed Sox17 transcription factor [14]. Ectoderm is outer layer and able to develop nervous system and retinoic acid (RA) drives to ectoderm [15]. Mesoderm is the middle layer characterised by expressing T box t (Brachyury) and develops muscle, cartilage, bone, and blood cells as indicated in Figure 1.2. They are sourced embryonic cells, so they are isolated from inner cell mass of preimplantation blastocyst [16].

There are three types of pluripotent stem cells; embryonic stem (ES) cells, embryonic germ cells and induced pluripotent stem cells (iPSCs). Firstly, ES cells are derived from mouse, non-human primates and human. They are characterized by expression of Oct4, Klf4, Sox2, c-myc, and Nanog. Teratoma formation of immunodeficient mice is the *in vivo* pluripotency analysis [17]. Another pluripotency characterization analysis is that PSCs can construct embryoid body *in vitro* [18].

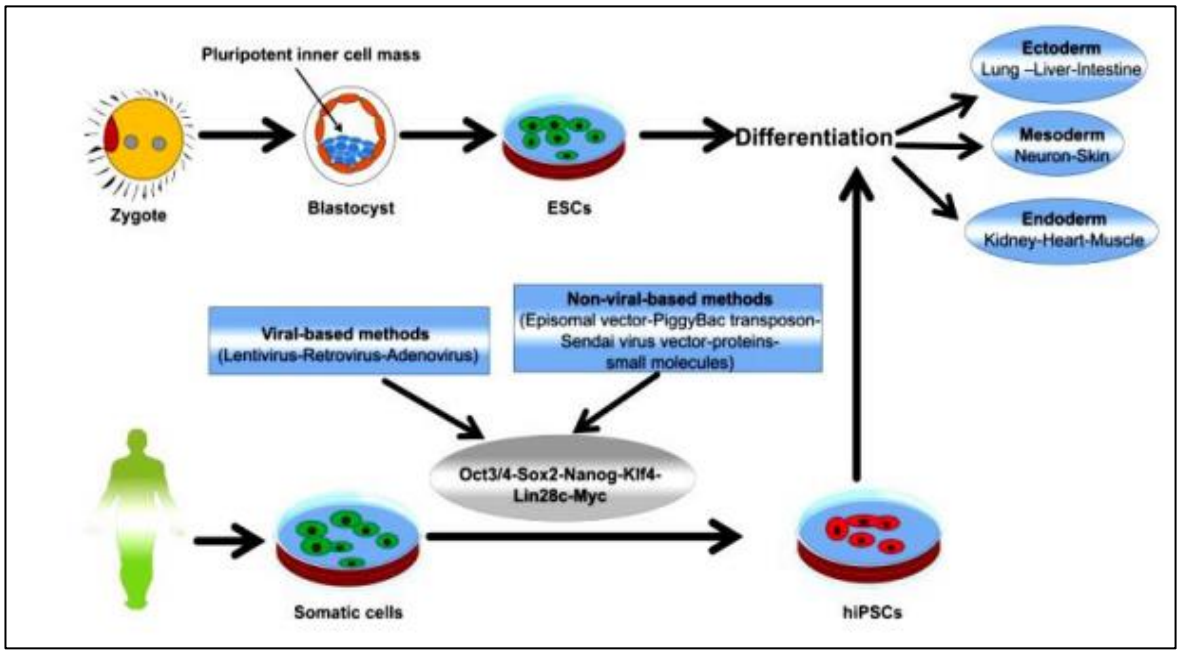

Figure 1.2. Schematic representation of derivation of Pluripotent stem cell and differentiation to three germ layer [20]

Murine ES cells were identified in early 1980s. They need to leukaemia inhibitor factor (LIF) or embryonic fibroblast to maintain pluripotent state. On the other hand, human ES cells were derived from blastocyst *in vitro* fertilization (IVF) in 1998 by Evans [21]. Some of new human ES cells line was discovered until 2004 and human ES cells can grow *in vitro* [6,22]. New standardizing protocol and medium conditions was developed. Human ES cells have some morphological differences from mouse ES cells [23]. In contrast, human ES cells do not need to LIF to maintain pluripotency state, they need to fibroblast growth factor 2 (FGF2) and activin A. Despite mouse ES cells express SSEA1 (stage specific embryonic antigen), human ES-cells express SSEA3, SSEA4, TRA1-60 and TRA1-81 [24]. Mouse ES cells are grown dome-shaped colonies but human ES cells colony appear a flatter *in vitro* [25].

1.3. INDUCED PLURIPOTENT STEM CELLS (iPSCs)

Induced pluripotent stem cells (iPSCs) are derived from adult somatic cells with cellular reprogramming. In 2006, mouse fibroblast developed to similar properties of ESCs [26]. In 2007, human fibroblast generates to human iPSCs with same approaches [27]. In 2006, introducing four genes that are Oct4, Sox2, Klf4 and c-Myc or Oct4, Sox2, Nanog and LIN28 [28]. The transcription factors target the stemness, they are used to reprogram of potency. Reprogramming based on oncogenes such as Klf4 (Kruppel-like factor 4) or c-myc [29] that affect the downregulation of genome stability such as p53. Oct4 is another transcription factor that is specific to early embryogenesis and expressed in oocytes, early embryo, embryonic carcinoma cells, and mouse ES cells [30]. In addition, Nanog was the first described transcription factor provide to maintain self-renewal and pluripotency of ES cells. It expresses in the interior cells of the compacted morula and the ICM of the blastocyst [31].

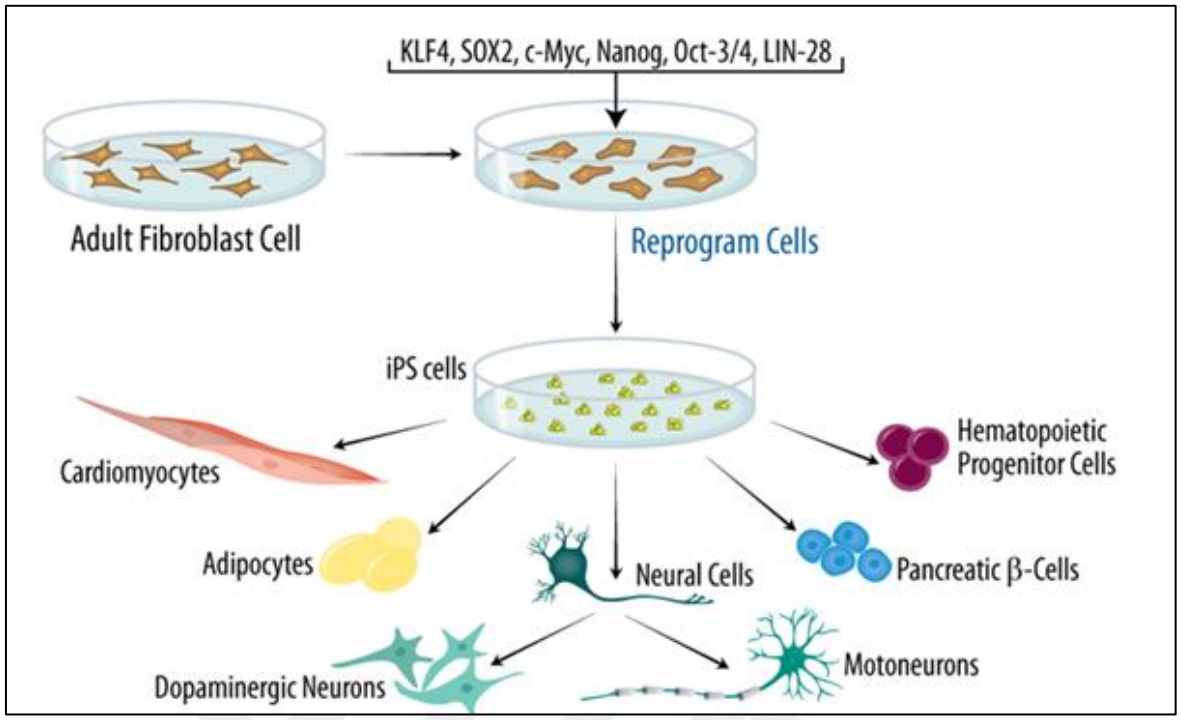

Figure 1.3. Reprogramming of iPSCs technology [29]

Generating of iPSCs are divided into two methods are non-viral and viral integration. iPSCs were generated efficiently using retroviruses and lentiviral integration but it has high risk of mutation potential [32]. Moloney murine leukemia virus (MMLV)-derived retroviruses are used to generate iPSCs. In comparison other methods, the retroviral vectors such as pMSCV can infect dividing cells and most efficient iPSC generated but it has highly mutagenesis and integrate randomly. Therefore, it is not available for clinical application. Additionally, lentiviral vectors can also infect dividing cells and non-dividing cells. Thus, it has high capacity than retroviral vectors. The non-viral methods are based on delivery of DNA, RNA and protein. DNA delivery for reprogramming is transfected plasmid [29]. Another method is RNA-based methodology reduces mutagenesis and genomic integration and more efficient. However, generating the modified mRNAs are more difficult than other methods [33].

In regenerative medicine, using of iPSCs is targeted to neurodegenerative disease treatment such as Parkinson disease, Alzheimer and spinal cord injury [33,34]. In addition to these, they can be used a toxicology test of cardiac myocytes and hepacytes [11]. Furthermore, iPSCs can be used in genetic engineering of monkey, porcine and canine to generate disease model and production of enzyme [35–37].

1.4. NEUROMESODERMAL PROGENITORS

The central nervous system (CNS) is the constructed of epiblast cells in front of the anterior primitive steak or is known as an anterior neural plate. In vertebrates, the forebrain assembles in the rostralmost part of this region, but the midbrain and hindbrain appear closer to the primitive streak or known as (CLE). Consequently, the head and trunk nervous systems are different from developmental origins. Epiblast rostral to the primitive streak have head or neural progenitors that give rise to brain. On the other hand, trunk and posterior neural tissue progenitors that develop hindbrian and spinal cord-derived from the anterior region of the primitive streak or the caudal lateral epiblast (CLE) and node streak border (NSB) [39]. The trunk of the mammalian embryos contains an endoderm, spinal cord and different types of mesoderm axial, paraxial, intermediate and lateral plate. Two types of progenitor cells have the responsible of the development of this region [40]. One of them is the node that can be derived from axial mesoderm [41] and another one is Neural mesodermal progenitor (NMPs) which is bipotent stem cells that give rise to paraxial mesoderm and spinal cord. The node and NMPs population is associated with the caudal epiblast (CE) in the embryo [42].

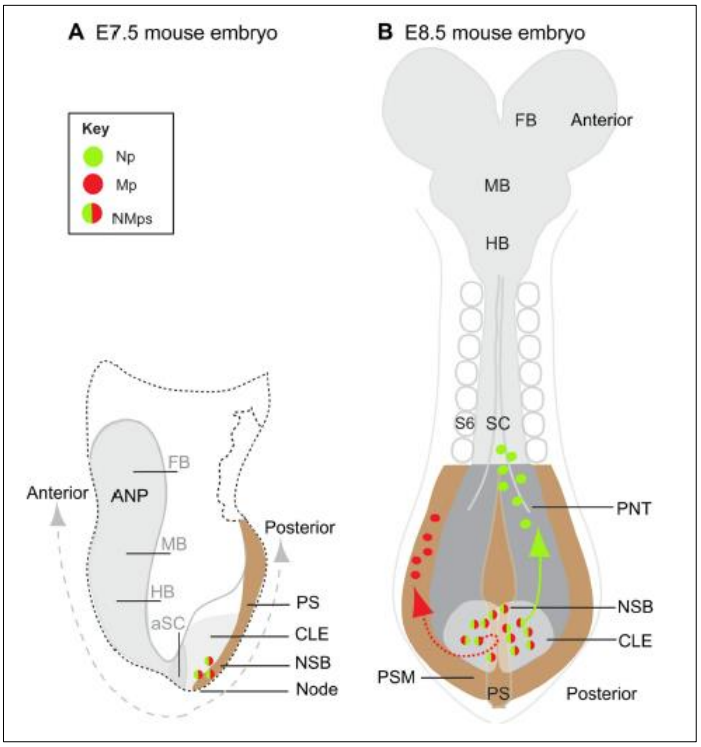

Figure 1.4. Localization of progenitor cells of mouse embryo embryonic day 7.5 and 8.5 [42]

In mouse and chick embryos, NMPs appear in the developing tail and trunk. Trunk NMPs are located in the caudal lateral epiblast and the node streak border and the tail NMPs are located in chordo neural hinge (CNH) while embryonic day (E) 8.5. as indicated Figure 1.4.

Three pathways play role in NMP fate, Wnt pathway, Fibroblast growth factor (FGF) pathway and RA as shown as Figure 1.5.. When Wnt and FGF are balanced with RA, maintain NMP state as shown as Figure 1.4.2 [38,43]. Although Wnt and FGF pathways drives mesoderm, RA drives neural fate. At the same time, NMPs are distinguished by the coexpression of the T box factor T (Brachyury) and the neural factor Sox2, this balance causes maintain NMPs bipotent state. Wnt signalling maintain activation of both T and Sox2 [44].

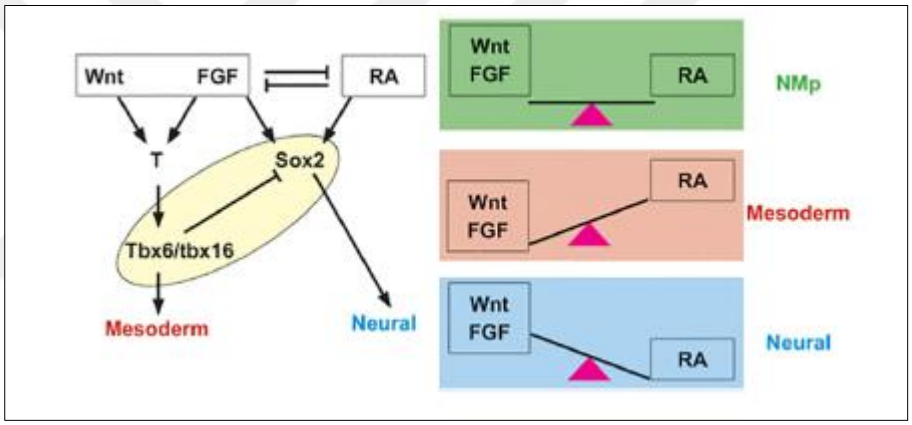

Figure 1.5. Maintaining factor of Neuromesodermal progenitors [44]

1.5. SPINAL CORD NEURONS DEVELOPMENT

During embryonic development in vertebrates, the dorsal mesoderm constructs notochord that is a rod extend to dorsal side of embryo. Therefore, mesodermal cells secrete some signalling molecules results the neural plate from the notochord above the ectoderm [45]. Neural tube give rise to spinal cord and CNS [46].

Inhibition of Bone morphogenetic protein (BMP) signalling induce neural cell fate [42,46]. Noggin, Chordin and Follistatin inhibit BMP4 and give rise to neuroectoderm [47,48]. RA and FGF can trigger neural tube formation that forms embryonic CNS consist of forebrain, midbrain, hindbrain and spinal cord as indicated in Figure 1.6.A [50]. Together with these signals sonic hedgehog morphogen (Shh) secreted by notochord increases ventral to dorsal gradient. Moreover, RA expression promotes rostral motor neurons called as rostralizing and FGFs promote caudal motor neurons called as caudalizing [51].

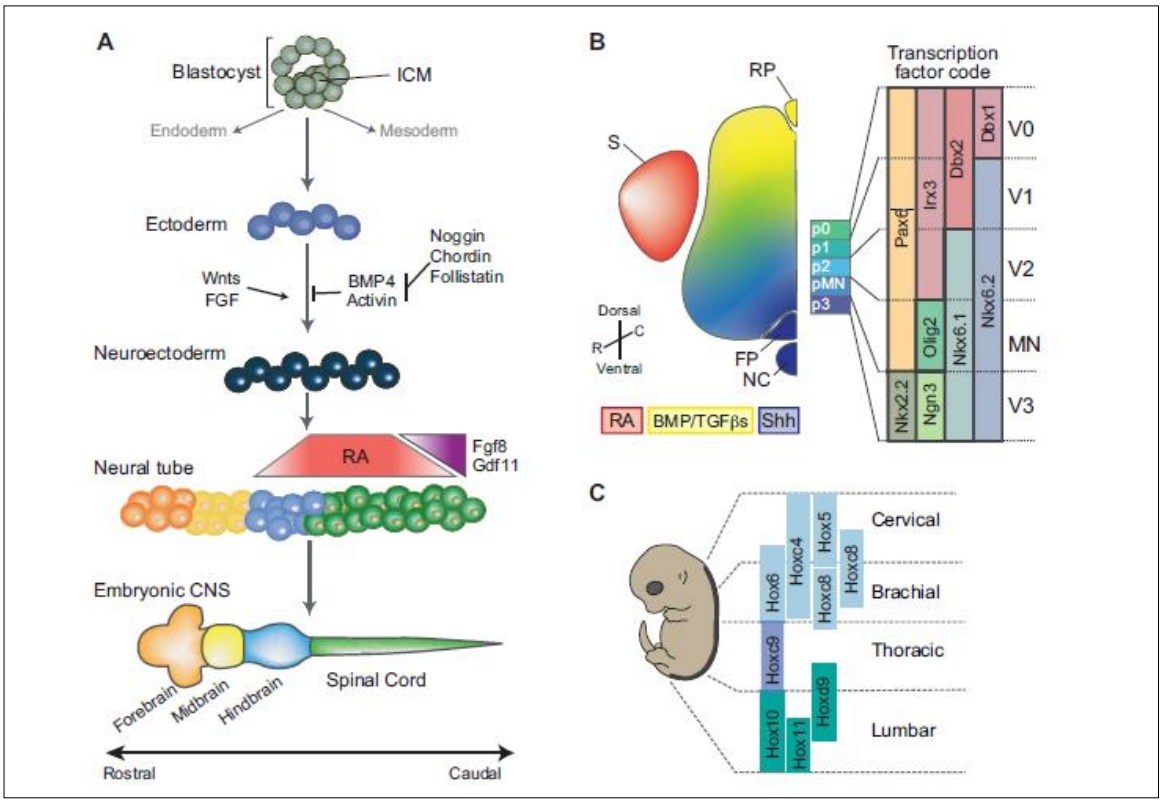

Figure 1.6. Development of Spinal Cord Neuron A. Development scheme of spinal cord from blastocyst. B. Spinal cord progenitor types and their transcription factors. C. Part of spinal cord and expressed transcription factors [50]

Shh also produced of five ventral progenitor cell domains that are p0, p1, p2, pMN, and p3. Each one can express different transcription factor that give rise V0-V3 interneurons and motor neurons. pMNs are motor neuron progenitors express Pax6, Olig2, Nkx6.1 and Nkx6.2 [50].

Hox gene family play an important role in development of spinal cord neuron [51]. Hox genes have four chromosomal clusters: HoxA, HoxB, HoxC and HoxD and each clusters has

13 paralogous subsets [51,52]. Anatomically, spinal cord has four regions that are cervical, brachial, thoracic and lumbar. Transcription factor Hoxc4, Hox5, Hoxc8 and Hox6 promote cervical and branchial spinal cord, Hoxc9 expressed in thoracic spinal cord Hox10, Hox11 and Hoxd9 lumbar part of spinal cord that indicates Figure 1.5C [50,53].

1.6. MOTOR NEURONS

Motor neurons (MNs) are also known efferent neurons are the nerve cells that are the part of central nervous system (CNS). They have a role of carrying impulse CNS to muscle cells indicates in Figure 1.7. MNs are responsible for all voluntary and involuntary movements [55]. Basically, motor neurons provide to move, swallow, breathe, talk, and eat. Ventral neural tube progenitors give a rise MNs and these progenitors generate oligodendrocyte precursors cells [56].

Motor neurons are divided into two main groups which are the upper MNs that compose cerebral cortex. Another one is lower MNs originate brainstem and spinal cord [57]. Upper MNs are placed in cortex of the brain and brainstem. Upper motor neurons are glutaminergic, whereas lower MN secrete neurotransmitter of acetylcholine [58].

Lower MNs can be seen in the spinal cord and are responsible for directly signal transduction to organs, glands and skeletal muscles. Lower motor neurons have also four subtypes which are special visceral efferent motor neurons, somatic motor neurons, and general visceral motor neurons. Somatic motor neurons are responsible for movement [59].

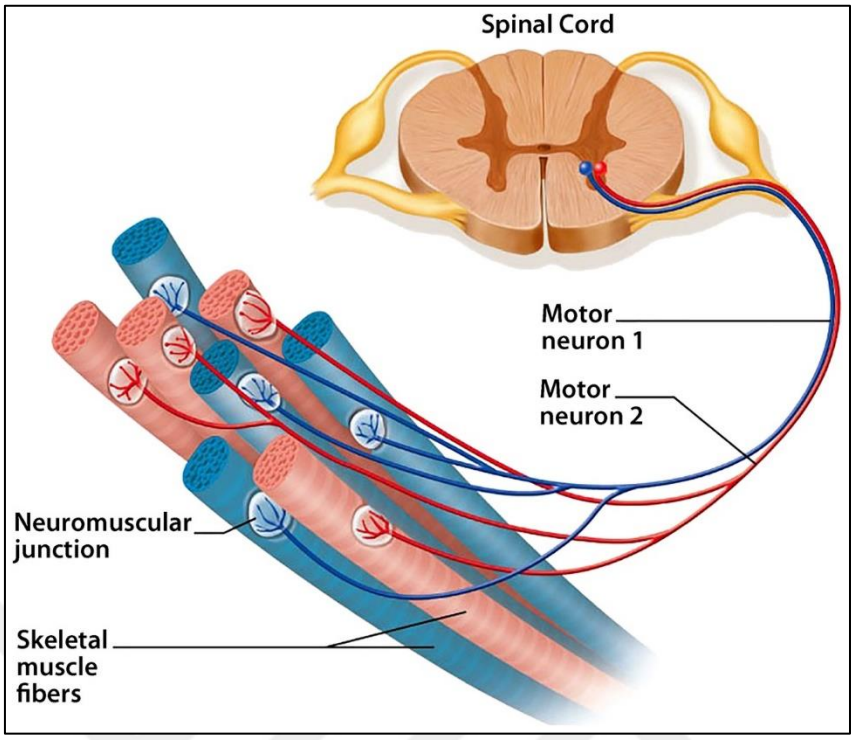

Figure 1.7. Schematic representation of motor neurons and muscle interactions [59]

1.7. MOTOR NEURON DISEASES

Motor neuron diseases (MND) are the type of neurodegenerative diseases that result in destroying both upper and lower motor neurons. These cells have a role of skeletal muscle activity such as walking, breathing, swallowing. MND is classified into four phenotypes: Spinal muscular atrophy (SMA), Amyotrophic lateral sclerosis (ALS), progressive bulbar palsy, and progressive muscular atrophy [60].

Spinal muscular atrophy (SMA) is genetic neurodegenerative diseases results from degeneration of motor neurons in spinal cord [61]. Since it is an autosomal recessive diseases cause deletion, conversion or mutation gene of survival motor neuron 1 (SMN1) [62–64]. Clinically, SMA is classified into four kinds based on the age of diagnosis [64].

Type I SMA disease also known Werdnig-Hoffmann disease is the most common type of SMA. Half of SMA patient is diagnosed with type I. It indicates before 6 months of age and death the first two years of life. The patients cannot sit without support and cannot head control. They have trouble to swallowing and have spared diaphragm. Therefore, patients have problems with airway protection and have a risk of pneumonia [65,66].

Type II SMA diseases patients' onset between 7-18 months. Most of the patients can sit but none of them stands and walks independently. Some patients have kyphoscoliosis that required surgical intervention [67].

Patients of type III are characterised onset after 18 months and patients indicate profound symptom heterogeneity. For instance, some of the patients need a wheelchair some of them can walk and live adult lives. Patients with type III SMA develop scoliosis. Lastly, type IV patient of SMA shows symptoms in the 20 years or 30 years of life [64,67].

ALS is also known classical motor neuron disease that affect both upper and lower motor neurons [16]. ALS is fatal diseases that lead to loss of muscle control. Early symptoms of ALS are muscle weakness or stiffness in bulbar muscles. Therefore, patients have trouble to eat, speak and finally breathe [68]. Within 3-5 years of receiving an ALS diagnosis, patients die from respiratory failure. 10 percent of patients is familial and other one is sporadic. Rosen was demonstrated that Superoxide dismutase 1 (SOD1) gene mutation establish 20 percent of familial ALS. There are 90 different types of SOD1 mutations. Furthermore, different mutations show different symptoms. Moreover, some environmental factors cause ALS. Neurologists detect that mercury, arsenic and lead in the blood and urine leads to ALS [69].

1.8. CELL THERAPY FOR MOTOR NEURON DISEASES

Cell therapy targets to introduce healthy cells into patients' body that replace mutated or missing cells. Stem cell therapy has been developed for the treatment of both SMA and Amyotrophic lateral sclerosis (ALS). Differentiation potential is demonstrated by embryonic stem cells, neural progenitor cells (NPCs), neural stem cells, and mesenchymal stem cells (MSCs) [70]. Although, ES cells can differ to three germ layers, MSC and NPCs have restricted differentiation capacity. Therefore, ES cells can be used to therapy for motor neuron disease. However, isolation of MSCs is easy and MSCs are more abundant than other cell types [56]. Because of their potential to move into injured brain regions and stimulate neurogenesis, multipotent stem cells can be an appealing therapeutic alternative. Stem cell therapy can be approached in two ways. to help motor neuron diseases. One of them is using progenitor cells ex vivo to generate neuronal cells [72]. Patient-specific induced pluripotent stem cells therapy is a powerful treatment for motor neuron diseases such as ALS and SMA. iPSCs obtain from the patient's fibroblast cells by skin biopsy. Then generating iPSCs used

by Yamanaka's factor cocktail and further iPSCs generate motor neurons [56]. The second approach is promotion of the survival of existing cells. MSCs are appropriate cell types for cell therapy due to their plasticity and immunomodulatory properties [72]. MSCs can release cytokines and chemokines that promote survive or neurons [73].

1.9. AIM OF THE STUDY

The aim of the project is to establish fully functional motor neurons from human induced pluripotent stem cell via an intermediate NMP progenitor cell population. In the current study, we aimed to generate an ex vivo protocol to obtain spinal cord motor neurons from their embryonic origin cells.

2. MATERIAL AND METHODS

2.1. iPSC GENERATION AND CELL CULTURE

iPSCs were derived from human fibroblast cells (HDFCs) previously in our laboratory and used in this project. Briefly, HDFCs were reprogrammed into iPSCs with StemRNA 3rd Gen Reprogramming Kit (ReproCELL, USA) at passage 7 using Lipofectamine RNAiMAX (#13778150, Invitrogen, USA) based on manufacturer's instructions [74]. iPSCs were cultured in mTESR medium (#85850, StemCell Technologies, Canada) on hESC-qualified Matrigel (#356230, Corning, USA) coated 6-well plates and incubated at 37°C and 5 percent CO_2 in an incubator. The medium of cells was replaced each day.

2.1.1. Live Alkaline Phosphatase (ALP) Activity

iPSCs were rinsed with DMEM/F-12 media (#11320033, Gibco, UK). 500X stock Alkaline phosphatase live stain solution (#A14353, Thermo Fischer, USA) was diluted in DMEM/F-12 medium and applied onto adherent iPSCs based on the manufacturer's protocols [75]. The iPSCs have been incubated with ALP dye for 20 minutes in the incubator at 37°C and 5percent CO_2 in atmosphere and then washed with the DMEM/F-12 media twice to remove excess dye. After that, iPSCs were visualized under fluorescent microscopy (Axio Vert.A1; Zeiss, Germany) equipped with AxioCam ERc5s camera. Images were captured 30 minutes after staining and positive colonies were selected in Zen 3.3 blue edition software (Carl Zeiss Microscopy, NY, USA).

2.1.2. Trilineage Differentiation

iPSCs can differentiate into endoderm, ectoderm, and mesoderm lineages. iPSCs were seeded onto hESC qualified matrigel coated 12 well-plate and treated with STEMdiff™ Trilineage Differentiation Kit (#05230, StemCell Technologies, USA) [76]. Endoderm and mesoderm induction media were applied for 5 days while ectoderm media was applied for 7 days. After differentiation, cells were immunostaining with Pax6 (mouse, #sc-12721, SantaCruz Biotechnologies, USA), Sox17 (rabbit, #NBP2-24568, Novus Biological, USA)

and T/Bra (mouse, # sc-374321, SantaCruz Biotechnology, USA) and visualized under fluorescent microscopy (Axio Vert.A1; Zeiss, Germany) equipped with AxioCam ERc5s camera.

2.1.3. Chromosome Abnormality

Genomic DNA was isolated from iPSCs with a High Pure Genomic DNA Purification Kit (#11796828001, Roche, USA). Then, a qPCR-based hPSC Genetic Analysis Kit (#07550, STEMCELL Technologies, USA) was used for the detection of the karyotyping abnormalities in iPSCs according to the manufacturer's procedures.

2.2. DERIVATION AND CHARACTERIZATION OF NEUROMESODERMAL PROGENITORS (NMPS)

iPSCs were harvested with Versene solution and seed on the low attachment 24-well plate at the $2x10^5$ cells per well in N2B27 (3 μM CHIR99021 (#72052, StemCell Technologies, Canada), 12 ng per ml bFGF (#100-18B, Peprotech, UK) and 10μM ROCK inhibitor Y-27632 (#72302, StemCell Technologies, Canada)) for 3 days according to the previously published protocol with minor modifications [77]. N2B27 medium is a serum free medium for generation of embryoid bodies which consists of a ratio of 1:1 DMEM-F12 medium and Neurobasal medium (#21103049, Gibco, UK) 0.5percent N2 supplement (#17502048, Gibco, UK), 1 percent B-27 supplement (#A3582801, Gibco, UK), 0.5percent of Bovine serum albumin (BSA, #A1595, Sigma, USA), 1 percent L-glutamine (#G7513, Sigma, USA) and 1 percent penicillin- streptomycin- and amphotericin B (PSA, #15240062, Gibco, UK).

2.2.1. Characterization of NMPs by Immunocytochemistry

NMPs were seeded on Matrigel-gelatine coated eight well chamber (30108, SPL, Korea) and incubated at 37°C and 5 percent CO_2 in a humidified incubator. They have been fixed with 4 percent paraformaldehyde (PFA) for 30 minutes and permeabilized in 0.1percent Triton-X (#X100, Sigma, USA) in PBS for 5 minutes. Then, NMPs were washed with PBS-Tween20 and blocked with 1percent BSA for 40 minutes. After that, NMPs were incubated

with the following primary antibodies Sox-2 (mouse, #sc-365823, SantaCruz Biotechnology, USA), T/Bra (mouse, #sc-374321, SantaCruz Biotechnology, USA), Apelin Receptor (mouse, #702069, Invitrogen), β-catenin (rabbit, #8480s, Cell Signalling Technologies), Active β-catenin (rabbit, #8814S, Cell Signalling Technologies for overnight at 4˚C. After that, NMPs were rinsed and incubated with secondary antibodies consist of AlexaFluor 488 (anti-mouse, #4408S, Cell Signaling Technology, USA) and AlexaFluor 647 (anti-rabbit, #4414S, Cell Signaling Technology, USA) for 40 minutes at the room temperature. For nuclei staining, DAPI (1:10000; # A1001.0010, Applichem, Germany) was used in the secondary antibody. The pictures of samples were visualized using a confocal microscope (LSM 700; Zeiss, Heidelberg, Germany). Finally, using the Zen 2011 software density measurements of staining was calculated. The results were converted into graphs by statistical analysis using the GraphPad Prism 8 software (GraphPad Software, San Diego, CA, USA).

2.2.2. Characterization of NMPs by qPCR

Total RNAs were isolated using Trizol solution (#T9424, Sigma, USA) based on the manufacturer's instructions. cDNA was synthesized by a High-Capacity cDNA Reverse Transcription kit (#4374967, ThermoScientific, USA). Primers (Table 2.2.2) have been designed by software of Primer-BLAST from the National Center for Biotechnology (Bethesda, MD, USA) and they were synthesized by Sentegen (Ankara, Turkey). For normalization, β-actin was employed as a housekeeping gene. SYBR green method was applied to determine gene expression. 1 µl of synthesised cDNA (1000ng/ml) were mixed with primers, SYBR-mix (#K0221, Fermentas, USA) and PCR grade distilled water (#SH30538.02, Hyclone, USA). CFX96 qPCR system (Bio-Rad, Hercules, CA) was utilized in all qPCR experiments.

2.3. DIFFERENTIATION OF NMPS INTO SPINAL CORD NEURONS

NMPs were plated at cells on Matrigel-gelatin (1:200) coated 100 mm petri dishes in N2B27 medium supplemented with 0.1 μM Retinoic Acid (RA, #ab120728, Abcam, UK), 0.5 μM SAG dichloride (SML1314, Sigma Aldrich, Merck, Germany) and 10μM ROCK inhibitor for 2 days. After that, the cells were plated on Matrigel-gelatin coated 100 mm petri dishes in N2B27 medium consist of 0.1 μM RA and 50 ng per ml Shh for 2 days. The cells were plated on Matrigel-gelatin coated 100 mm petri dishes in N2B27 medium containing 0.1 μM Retinoic acid and 50 ng per ml Sonic hedgehog for a day. Then, the cells were plated on Matrigel-gelatin coated 100 mm petri dishes in N2B27 medium supplemented with 0.1μM RA and 50 ng per ml Shh and 10 ng per ml bFGF (#100-18B, Peprotech, UK). Until the end of 40 days differentiation protocol was shown as Figure 2.3.

2.4. CHARACTERIZATION OF SPINAL CORD NEURONS

2.4.1. Morphology Analysis

The morphologic change in the neuron differentiation culture was monitored by light microscope images taken during differentiation protocol with an inverted microscope (Nikon Eclipse, TE200) equipped with Nikon Eclipse, TE200 camera using NIS Elements BR 2.30 software program.

2.4.2. Immunocytochemical Analysis

iPSCs derived SC neurons were seeded on Matrigel-gelatine coated the eight well chamber at density of $5x10^3$ cells and incubated at 37°C and 5 percent CO_2. They were fixed with 4 percent PFA for 30 minutes and permeabilized in 0.1percent Triton-X (#X100, Sigma, USA) in PBS. Then, iPSCs derived SC neurons were washed with PBS and blocked with 1percent BSA for 40 minutes. Afterwards, cells were incubated with primary antibodies Sox2 (rabbit, #3579, Cell Signalling, USA), NeuroD1 (mouse, #ab60704, Abcam, UK), MAP2 (rabbit, #45425, Cell Signaling, USA), NEFH (mouse, #13-1300, Thermo Scientific), β-tubulin III (rabbit, #ab18207, Abcam, UK), Islet1 (mouse, #ab86472, Abcam, UK) and Islet2 (rabbit,

#176576, Cell Signaling, USA), Neun (rabbit, #ab177487, Abcam, UK), Pax6 (mouse, #sc-12721, SantaCruz Biotechnologies, USA), Mnx1 (rabbit, #ab92606, Abcam, UK)for overnight. After that, iPSCs derived SC neurons were washed with PBS-Tween20 and incubated with secondary antibodies including AlexaFluor 488 (anti-mouse, #4408S, Cell Signaling Technology, USA) and AlexaFluor 647 (anti-rabbit, #4414S, Cell Signaling Technology, USA) for 40 minutes at the room temperature. For nuclei staining, DAPI (1:10000) was used with secondary antibody. The pictures of samples were captured using a confocal microscope Zen 2011 software was used for staining density measurements.

2.4.3. Quantitative Real-Time PCR Analysis

Total RNAs were isolated using Trizol solution according to manufacturer's protocol. cDNA was synthesized by HighCapacity cDNA Reverse Transcription kit (#4374967, ThermoScientific, USA). Primers had been designed by software of Primer BLAST from the National Center for Biotechnology and synthesized by Sentegen. For normalization, β-actin was employed as a housekeeping gene. SYBR green method was applied to determine gene expression. 1 µl of synthesised cDNA (1000ng/ml) were mixed with primers, SYBR-mix (#K0221, Fermentas, USA) and PCR grade distilled water (#SH30538.02, Hyclone, USA). CFX96 qPCR system (Bio-Rad, Hercules, CA) was utilized in all qPCR experiments.

Table 2.1. Primers used in qPCR analysis for NMP characterization

Gene	Species	Primer Sequence
β-Actin	Human	F 5’GACAGGATGCAGAAGGAGATTACT 3’ R 5’TGATCCACATCTGCTGGAAGGT 3’
AR	Human	F 5'GGCCAGTGGCCAATGCTC 3' R 5'AGGGCATCCAGCACAGGG 3'
Wnt3a	Human	F 5’ TCAGCTGCCAGGAGTGCACG 3’ R 5’ CGCCCTCAGGGAGCAGCCTAC 3’
Sox-2	Human	F 5’ GGGAAATGGGAGGGGTGCAAAAGAGG 3’ R 5’TTGCGTGAGTGTGGATGGGATTGGTG 3’
T/Bra	Human	F 5’ TATGAGCCTCGAATCCACATAGT 3’ R 5’ CCTCGTTCTGATAAGCAGTCAC 3’
Nkx1-2	Human	F 5’ CCCTCCCACCACAAGATTTCT 3’ R 5’ GACCTCCGCCAAACTTTTCCT 3’
Mixl-1	Human	F 5’CTGTGCTACTGAAA 3’ R 5’ TGGGAGCAGAGATG 3’
PDGFR	Human	F 5’TCAGCTACAGATGGCTTGAR 3’ R 5’GCCAAAGTCACAGATCA 3’

Table 2.2. Primers used in qPCR analysis for Spinal Cord characterization.

HOXA4	Human	F 5’ GTTGCCACCCAAGAGAGAAC 3’ R 5’ CCAAGTAGTCCTTCTCAGGTATCC 3’
B-Tubulin	Human	F 5’ GCAACTACGTGGGCGACT 3’ R 5’ CGAGGCACGTACTTGTGAGA 3’
NeuroD1	Human	F 5’ GGATGACGATCAAAAGCCCAA 3’ R 5’ GCGTCTTAGAATAGCAAGGCA3’
Neurog2	Human	F 5’ AGGAAGAGGACGTGTTAGTGC 3’ R 5’ GCAATCGTGTACCAGACCCAG 3’
Tuj1	Human	F 5’ GGCCAAGGGTCACTACACG 3’ R 5’ GCAGTCGCAGTTTTCACACTC 3’
MNX1	Human	F 5’TTACCTGACTTATGAAACTTGAAACC 3’ R 5’CCCAGAGACGTAAGCATAAACC 3’
ISL1	Human	F 5’ AAACAGGAGCTCCAGCAAAA 3’ R 5’ AAAGGACTCTTTCAGCCAAGG 3’
Pax3	Human	F 5’ ATTGGCAATGGCCTCTCA 3’ R 5’ AGGGGAGAGCGCGTAATC 3’
Pax6	Human	F 5’ GCACACACACATTAACACACTTG 3’ R 5’GGTGTGTGAGAGCAATTCTCAG 3’
NKX6.1	Human	F 5’ GAGATGAAGACCCCGCTGTA 3’ R 5 ‘GACGACGACGAGGACGAG 3’
NKX6.2	Human	F 5’AGCACAAACCCTCGAACTTG 3’ R 5 ‘CCCGGATTCTGCAAAAATAG 3’
NKX1/2	Human	F 5’ GTCGAAGCGGGGAAAGAT 3’ R 5 ‘GATCCTCCGATCCTCCT 3’

2.4.5. Staining by Fluo-4 AM

iPSCs derived SC neurons were seeded on Matrigel-gelatin coated 24 well-plate. After a day, discarded medium and loaded Fluo-4 AM (#F10489, Invitrogen, UK) for 30 minutes incubated at 37˚C [78]. After the incubation, the iPSCs derived SC neurons were rinsed with PBS for 5 minutes. Then, iPSCs derived SC neurons were visualized in live-cell image microscope (Axio Observer, Zeiss, Germany) with Axicam 705 mono camera for 10 seconds intervals in 15 minutes. Fluo-4 intensity was measured on Zen 3.3 blue edition software and intensity results were converted into graphs by statistical analysis using the GraphPad Prism 8 software

2.4.6. Protein Profiling

Protein pellet was collected at day 0, day 3, day 15 and day 30. LC/MS analysis was performed for these days according to the previously published protocol in Kocaeli University [79]. Briefly, the proteins were run on 12 percent SDS-PAGE and the gel was stained with colloidal Coomassie Blue G-250 after fixation in 40 percent methanol containing 10 percent acetic acid. After the protein bands were cut, in-gel tryptic digestion was performed and the peptides were analyzed by nLC-MS/MS using Ultimate 3000 RSCL nanosystem (Dionex, Thermo Fisher Scientific, USA) coupled to a Q Exactive mass spectrometer (Thermo Fisher Scientific, USA). Xcalibur 4.0 software (thermo Fisher Scientific, USA) was used. Mobile phases A and B were used for high performance liquid chromatography (HPLC) and full-scan MS spectra were acquired. The top ten precursor ions were selected to perform MS/MS and the protein identification analysis were done using Proteome Discoverer 2.2 software (Thermo Fisher Scientific, USA) and searched against the database of Uniprot/Swissprot.

2.5. *IN VITRO* REGENERATION POTENTIAL

2.5.1. Myogenic differentiation of ASC Telo cells

ASC Telo cells (SCRC-4000, ATCC) were seeded on 12 well plate at $1x10^4$ cells per well with DMEM (#11965084, Invitrogen, Gibco, UK) low glucose. After one day of incubation, media was replenished by myogenic medic containing 5 percent (v/v) horse serum, 0.1 μM dexamethasone and 50 μM hydrocortisone (Sigma, St. Louis, MO, USA) in DMEM contains 10 percent FBS and 1 percent PSA.

Characterization of myogenic cells was conducted by MyoD (rabbit, sc760, SantaCruz Biotechnology, USA), Desmin (rabbit, #sc-14026, SantaCruz Biotechnology, USA), Myh (rabbit, sc20641, SantaCruz Biotechnology, USA) immunostaining. Additionally, morphologic pictures were captured by microscope

2.5.2. Establishment of Neuromuscular junction

Spinal Cord neurons were cocultured with myogenic cells in 10 ng per ml bFGF in N2B27 medium and myogenic medium with a 1:1 ratio and another well was cultured with 10 ng per ml bFGF in N2B27 medium contains 5 percent horse serum and 10 percent fetal bovine serum for neuromuscular junction formation. Myogenic cells were stained with PKH67 green cell labelling kit (#MINI67-1KT, Sigma Aldrich, Merck, Germany), SC neurons were stained with PKH26 red cell labelling kit (#MINI26-1KT, Sigma Aldrich, Merck, Germany). The cells were seeded on Matrigel-gelatin (1:200) coated 12 well plate and cells were incubated at 37 °C and 5 percent CO_2 for 4 hours. After that, the SC neurons were visualised in a live-cell image microscope (Axio Observer, Zeiss, Germany) with Axicam 705 mono camera for a day interval in 2 hours.

2.5.3. Co-culture

Spinal cord neurons were seed on 24 well plate and myogenic cells were seeded on 0.4 μm insert (354572, Corning, USA) with myogenic and 10 ng per ml bFGF in N2B27 medium with 1:1 ratio and another well was cultured with 10 ng per ml bFGF in N2B27 medium consist of 5 percent horse serum and 10 percent fetal bovine serum. The cells were incubated at 37 °C and 5 percent CO_2 for a day. After a day, cells were stained with crystal violet and the pictures were taken by a microscope (Axio Vert.A1; Zeiss, Germany)

2.6. AXON ELONGATION ANALYSIS

SC neurons (ganglions) were placed on 10 cm dish. The length of the neuron and its axon length was taken pictures by light microscope images taken during differentiation protocol with an inverted microscope (Nikon Eclipse, TE200) equipped with Nikon Eclipse, TE200 camera using NIS Elements BR 2.30 software program. Then, the length of the axon was measured in Image J software. Additionally, SC neurons were placed on 24 well plate. The axon length and axon networking was visualized in live-cell image microscope (Axio Observer, Zeiss, Germany) with Axicam 705 mono camera for a day interval in 15 minutes. The length of the axon networking was measured with Wimasis software, and the length of the neuron was measured on Zen 3.3 blue edition software

2.6.1. Transmission Electron Microscopy (TEM) and Scanning Electron Microscopy (SEM)

Spinal cord neurons were fixed with 2.5 percent glutaraldehyde and formaldehyde in PBS for 2 hours at room temperature. After fixation, the cells were rinsed by dH_2O two times for 10 minutes. Then, the sample was dropped on holey carbon films on 200 mesh copper grids (#AGS147, Agar Scientific) and washed three times water and deep the Uranyl acetate (#19485, TED PELLA, USA) and other sample were stained with methylamine tungstate negative stain (#A51036, Thermo Scientific). Then, Spinal cord neurons were visualized in TEM (Jem2100Plus, Axio, Zeiss, Germany) with 120 kV.

The dried samples were coated with gold-platinum with a 7.5 nm thickness by BALTEC SCD005 sputter on Leica EM ACE200 vacuum coater and the neurons were visualized by Zeiss Evo40 SEM (Zeiss, Heidelberg, Germany).

2.6.2. Immunocytochemistry

iPSCs derived SC neurons were seeded on Matrigel-gelatine coated the coverglass at the density of $5x10^3$ cells and incubated at 37°C and 5 percent CO_2 in a humidified incubator. They had been fixed with 4 percent PFA for 30 minutes at 4°C and were permeabilized in 0.1percent Triton-X in PBS for 5 minutes. Then, iPSCs derived SC neurons were washed with PBS-Tween20 and blocked with 1 percent BSA for 40 minutes. Afterwards, cells were incubated with a primary antibody with Synaptophysin (mouse, #ab8049, Abcam, UK) for overnight. After a day, cells were washed with PBS and treated with the secondary antibody of AlexaFluor 488 (anti-mouse) and for nuclei staining, DAPI was used for 30 minutes at room temperature. Then, iPSCs derived SC neurons were rinsed with PBS-Tween20 and cells were incubated with Alexa Flour 594 phalloidin (#A12381, Thermo Fischer Scientific) for 20 minutes. The cells were visualized by confocal microscopy.

2.7. CRYOPRESERVATION CAPACITY OF iPSCs DERIVED SPINAL CORD NEURONS

Mature motor neurons at day 30 were freeze by three different solutions. One of them is containing 20 percent FBS 10 percent DMSO, 70 percent 10 ng per ml bFGF in N2B27 media. Second one was containing 10 percent DMSO and 90 percent 10 ng per ml bFGF in N2B27 media. Third one was StemCell Banker (#11890, Amsbio, USA). After a week, the neurons were thawed and seeded on Matrigel coated 10 cm dish. Morphologic pictures were taken by with an inverted microscope (Nikon Eclipse, TE200) equipped with Nikon Eclipse, TE200 camera using NIS Elements BR 2.30. Then, neurons were freeze by FBS containing freezing media. After three weeks of freezing, neurons were thawed and seeded on Matrigel coated 10 cm dish. The morphologic pictures were taken for 5 days interval and measured calcium influx by Fluo-4.

2.8. MOUSE EMBRYONIC STEM CELLS DIFFERENTIATE INTO SPINAL CORD NEURONS

2.8.1. Cell Culture

R1, mouse embryonic stem cells, (SCRC-1036, ATCC) were cultured on embryonic fibroblasts (MEFs) which had treated mitomycin c (Sigma, USA) in DMEM supplemented with 15 percent ESC qualified FBS (Invitrogen, Gibco, UK), 1 percent PSA, 2 mM glutamax (Invitrogen, Gibco, UK), 1X nonessential amino acids (Invitrogen, Gibco, UK), and 100 U/mL LIF (Peprotech, UK) and incubated at 37 °C and 5 percent CO_2 atmosphere in an incubator.

2.8.2. Differentiation of mESCs to SC neurons via NMPs

R1 cells were trypsinized for 2 minutes and reseeded on the 10 cm dishes. Then, the cells were incubated for 30 minutes in an incubator to separate MEFs at 37 °C and 5 percent CO_2 atmosphere. Then, R1 cells were collected and seed on the low attachment 24-well plate at a density of $2x10^5$ cells per well in N2B27 medium contains 12 ng per ml bFGF and 10μM ROCK inhibitor for 2 days. After two days, medium was changed with N2B27 medium supplemented 12 ng per ml bFGF and 3 μM CHIR.

NMPs were plated at cells on Matrigel-gelatin (1:200) coated 100 mm petri dishes in N2B27 medium supplemented with 0.1μM Retinoic Acid, 0.5 μM SAG dichloride and 10μM ROCK inhibitor Y-27632 for 2 days. After Shh supplemented N2B27 medium for 2 days. After two days, the cells were plated in N2B27 medium supplemented 0.1μM RA, 50 ng per ml Shh, and 10 ng per ml bFGF supplemented N2B27 medium for a day. After a day, the cells were plated in in N2B27 medium supplemented 10 ng per ml bFGF until the end of 30 days differentiation protocol.

2.8.3. Characterization of mESCs derived SC neurons

2.8.3.1 Morphologic Analysis of mESC derived SC neurons

Morphologic pictures of mESCs derived SC neurons were taken at day 15 and at day 30 with an inverted microscope (Nikon Eclipse, TE200) equipped with Nikon Eclipse, TE200 camera using NIS Elements BR 2.30 software program.

2.8.3.2 Immunostaining of mESC derived SC neurons

mESCs derived SC neurons were seeded on Matrigel-gelatine coated the eight well chamber at the density of $5x10^3$ cells and incubated at 37°C and 5 percent CO_2 in a incubator. They have been fixed with 4 percent PFA and were permeabilized in 0.1 percent Triton-X in PBS. Then, mESCs derived SC neurons were washed with PBS and blocked by 1percent BSA for 40 minutes. Following that, mESCs derived SC neuorons were incubated with primary antibodies Sox2 (rabbit), NeuroD1 (mouse), MAP2 (rabbit), β-tubulin III (rabbit), Islet1 (mouse) and Islet2 (rabbit), Neun (rabbit), Pax6 (mouse), Mnx1 (rabbit) for overnight. After that, mESCs derived SC neurons were washed with PBS-Tween20 and incubated with secondary antibodies consist of AlexaFluor 488 (anti-mouse) and AlexaFluor 647 (anti-rabbit) for 40 minutes at room temperature. For nuclei staining, DAPI (1:10000) was used. The images of samples were captured using a confocal microscope. Zen 2011 software was used for staining density measurements.

2.8.3.3 Fluo-4 Staining

mESC derived cells were cultured on Matrigel-gelatin coated 24 well-plate. After a day, discarded medium and loaded Fluo-4 AM for 30 minutes incubated at 37˚C [78]. Then, the cells were rinsed with PBS for 5 minutes. After that, cells were visualized in live-cell image microscope with Axicam 705 mono camera for 10 seconds intervals in 15 minutes. Fluo-4 intensity was measured on Zen 3.3 blue edition software and intensity results were converted into graphs by statistical analysis using the GraphPad Prism 8 software.

2.9. STATISTICAL ANALYSIS AND SOFTWARE

All statistical analysis was performed by GraphPad Prism 8.0.0 for Windows (GraphPad Software, San Diego, California USA, www.graphpad.com). Two-way analysis of variance (ANOVA) with Tukey's post-hoc test was applied for statistical analysis values were accepted less than 0.05 and all experiments was performed triplicate. Additionally, axonal length analysis was performed Wimasis web site, neutrite outgrowth tool (Onimagin Technologies, Cordoba, Spain, www.wimasis.com). Confocal microscope analysis and Fluo-4 intensity analysis was performed using Zen 3.3 blue edition software. Additionally, Heat map and PCA of protein profiling was performed by Perseus software (V1.6.15.0, (https://maxquant.net/perseus/), protein interactions were detected by String website (https://string-db.org/), biologic process and found in tissue analysis were performed David websites (Laboratory of Human Retrovirology and Immunoinformatics,Fredrick, Maryland USA, https://david.ncifcrf.gov/) [80,81] and expressed common protein analysis was performed by Perseus but multiple Venn scheme was drawn by interactivenn website (www.interactivenn.net) [82]

3. RESULTS

3.1. iPSC CHARACTERIZATION

iPSCs were generated from HDFCs with StemRNA 3rd Gen Reprogramming Kit. They were characterized by immunocytochemistry analysis. The iPSCs were highly expressed Nanog, Oct3/4 and TRA1-60 and have not expressed SSEA-1 (Figure 3.1a). The iPSCs were staining with Alkaline phosphatase live stain. Alkaline phosphatase up-regulated in iPSCs. (Figure 3.1c). Telomerase activity was 3.5-fold high in iPSCs compared to positive control (Figure 3.1e). The PCR product of the telomerase assay was loaded on the agarose gel and the band of iPSC high density of positive control as indicated in Figure 3.1e. Another iPSCs characteristic analysis is chromosome abnormality which was detected with a qPCR-based hPSC Genetic Analysis Kit. Chromosome of 1q, 4p, 8q, 10p, 12p, 17q, 18q, 20q and X were analysed by qPCR. There was not significant fold change observed compared to control. Therefore, there was no chromosome abnormality of iPSCs. Moreover, iPSCs were differentiated into endoderm, mesoderm, and ectoderm layer with STEMdiff™ Trilineage Differentiation Kit and morphologic pictures of differentiated cells were taken and indicated in Figure 3.2. Differentiated cells were stained with Pax6, Sox17 and T/Bra. Ectoderm differentiated cells expressed Pax6. T/Bra was expressed on the mesoderm differentiated group and Sox17 was expressed on endoderm differentiated group (Figure 3.2c).

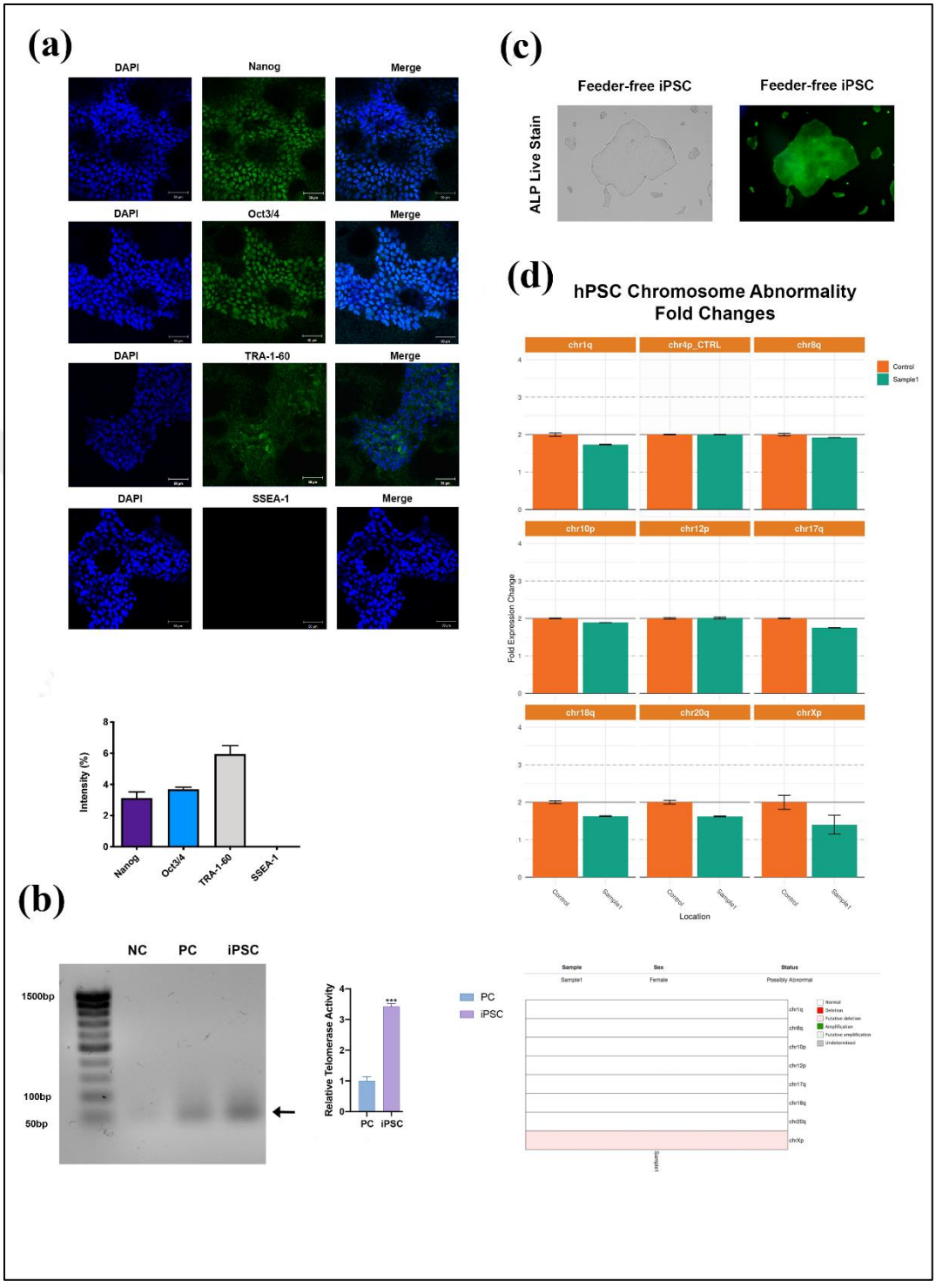

Figure 3.1. iPSCs were generated from HDFCs. (a) Immunostaining of iPSCs by Nanog, Oct3/4, TRA1-60 and SSEA-1, (b) Histogram graph of immunostaining of four markers, (c) ALP staining pictures, (d) Analysis of Chromosome abnormality

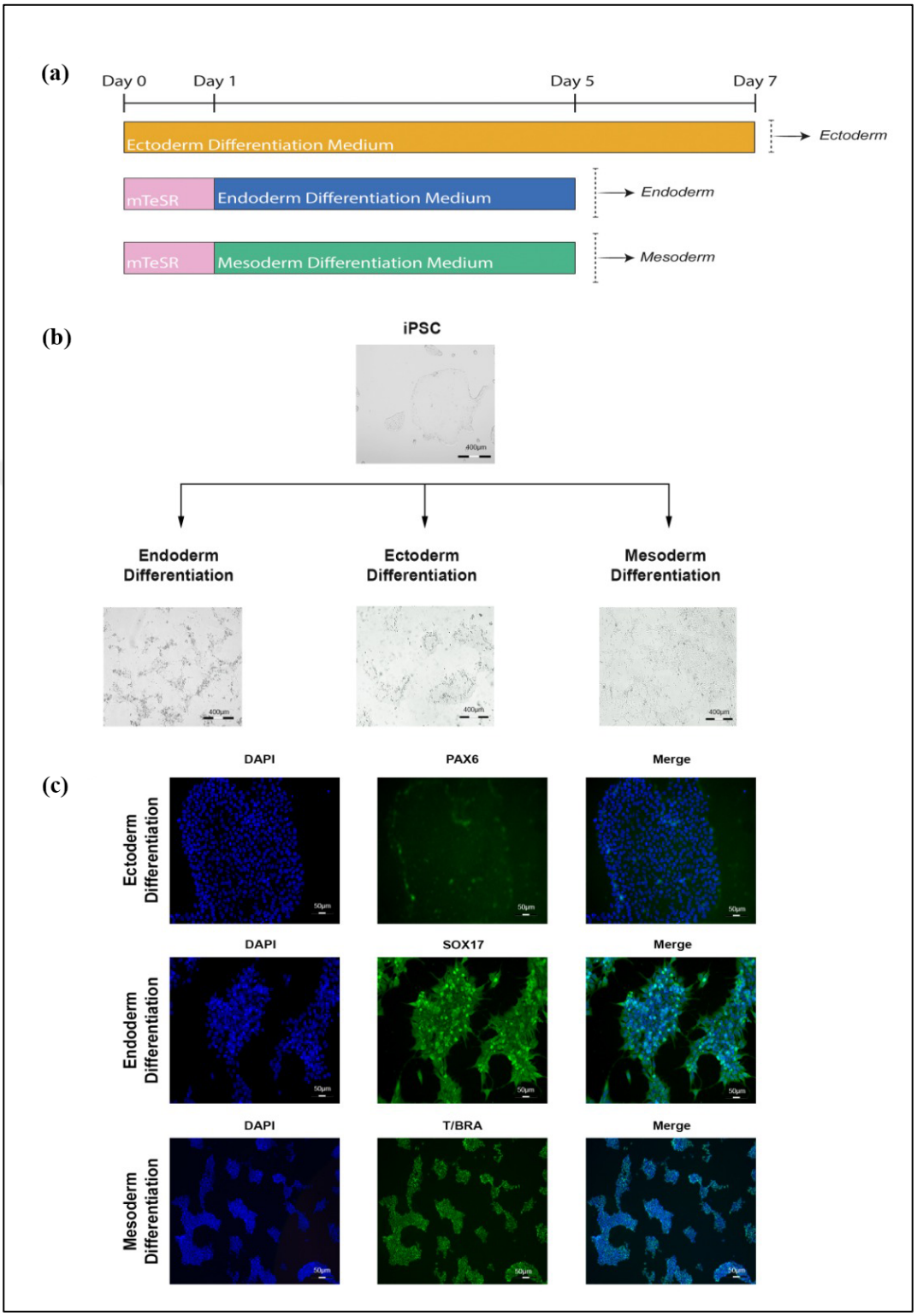

Figure 3.2. iPSCs were differentiated into three germ layers (a) Timeline of differentiation protocol (b) Morphological pictures of differentiated iPSCs (c) Immunostaining analysis of T/Bra, Pax6 and Sox17. Note: Scale bar: 50 µm

3.2. iPSCs DIFFERENTIATE INTO NMPS

iPSCs (Day 0) were differentiated to NMPs (Day 3) by treated bFGF and CHIR99021 which agonist WNT pathways for 3 days (Figure 3.3a). On day 3, Sox2 and T/Bra coexpressed NMPs were generated successfully (Figure 3.3b). Active β-catenin was expressed in NMPs and a mesodermal marker of apelin receptor expression was determined on NMPs. The gene expression of NMPs marker AR, T/Bra, Wnt3a increased 100-fold, Mixl-1, PDGFR and Nkxl-1 10-fold at Day 3 NMPs according to Day 0 cells. Additionally, Sox2, pluripotent and NMP marker, expression was not changed significantly as expected.

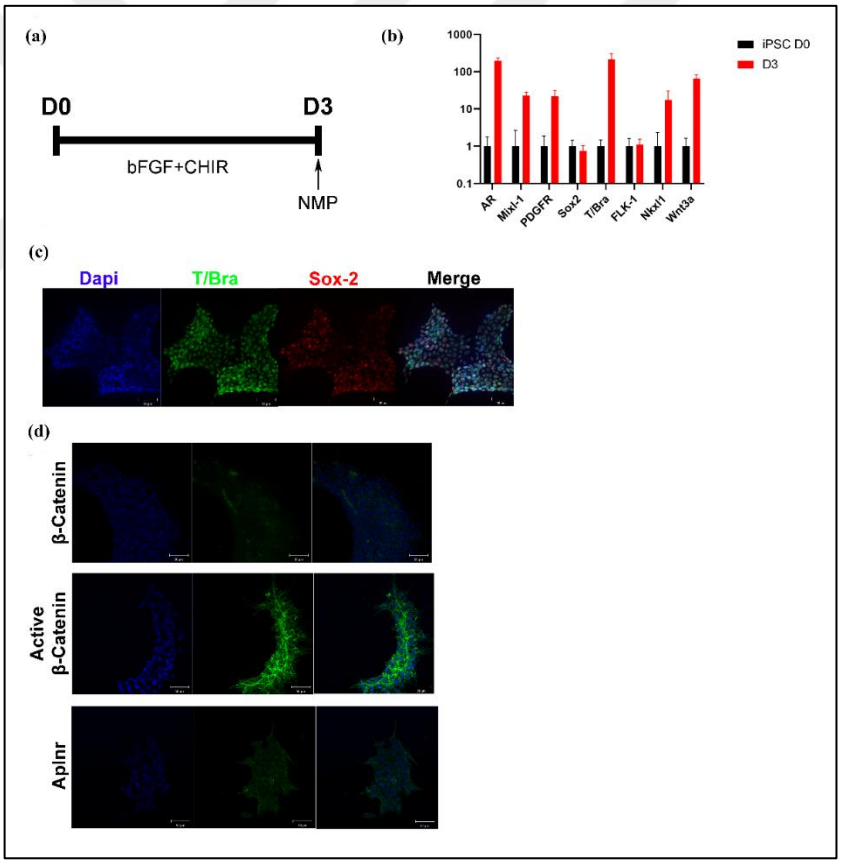

Figure 3.3. iPSCs were differentiated into NMPs. (a) Schematic representation of NMP differentiation protocol. (b) qPCR analysis of NMP markers. (c) Immunostaining analysis of T/Bra and Sox2 coexpression and Apelin Receptor, β-catenin and active β-catenin

3.3. DIFFERENTIATION OF NMPS INTO SPINAL CORD NEURONS

3.3.1. Morphological Analysis

The NMPs were differentiated into spinal cord neurons with 40 days differentiation period. NMPs (Day 3) were differentiated with 0.1 µM RA and 0.5 µM SAG for 2 days. After that, cells at Day 5 were differentiated with N2B27 medium supplemented with 0.1 µM RA and 50 ng per ml Shh for 2 days. Then, on day 7 cells were differentiated with N2B27 supplemented with 0.1 µM RA, 50 ng per ml Shh and 10 ng per ml bFGF for a day. After that, cells at Day 8 were differentiated with N2B27 supplemented with 10 ng per ml bFGF to Day 40 **(**Figure 3.4a**).** The morphologic pictures were taken at different time intervals during the differentiation protocol. On Day 3, the morphology of NMPs was the spherical embryoid body. The cells were spreading, and a spindle-like structure was observed on Day 5. Neuron like structure and axonal lengthen were determined on Day 10. In addition, branch structure was increased from Day 10 to Day 40 (Figure 3.4c).

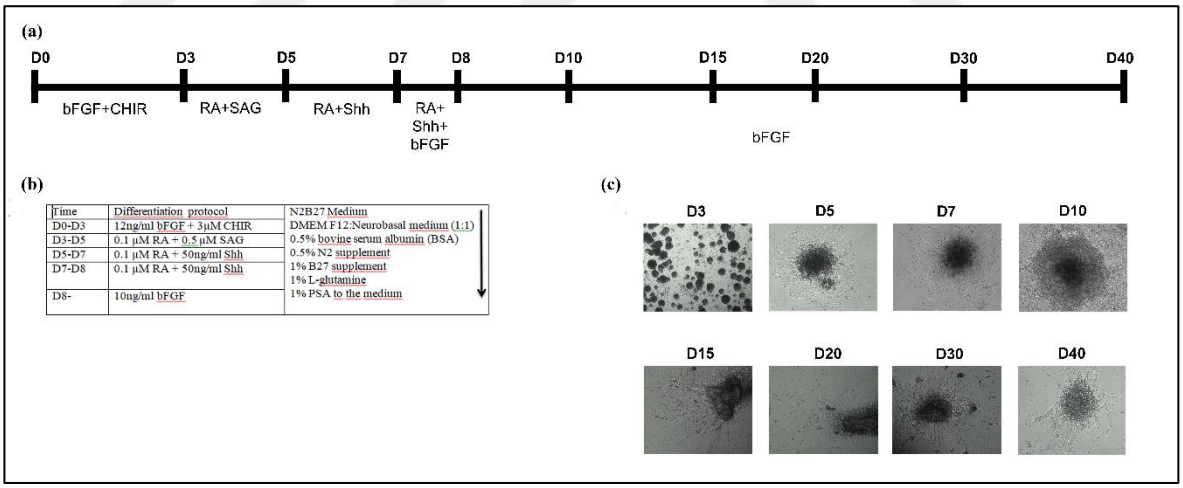

Figure 3.4. NMPs were differentiated to spinal cord neurons. (a) Schematic representation of the differentiation protocol of iPSCs. (b) Table of differentiation medium supplements (c) Light microscope images of differentiated cell. Scale bar 200 µm

3.3.2. Immunocytochemistry Analysis

Neural and neural progenitor markers expression was detected by ICC. A neural marker of β-tubulin is the part of tubulin, and it is also known tubulin III, it is highly expressed neural cells and provides to axonal transport and microtubule formation in body of neurons [83]. According to this, tubulin expression was expressed from Day 3 to Day 30. Neun, which stands for neuronal nuclei, is the neuron-specific nuclear protein [84,85] . Furthermore, Tyrosine Hydroxylase, TH, is the biosynthetic enzyme that play role in neurotransmitter synthesis. Thus, it is late marker. TH expression has increased from Day 3 to Day 30. Ventral/motor neuron progenitor can differentiate motor neurons [86]. The ventral progenitor marker of MNX-1 which is terminal transcription factor expression was increased 3-fold on Day 30 as indicated in Figure 3.5.

On the other hand, Sox2 is the expressed by NMPs expression was decreased dramatically from Day 3 to Day 30. The cells lost mesodermal fate until differentiation. Isl-1 and Isl-2 are the early marker of neurons which promote motor neuron differentiation [87], their expression was increased at Day 3 but it was diminished through Day 30. Otherwise, the motor neuron progenitor gene of PAX-6 which is the transcription factor of neurogenesis expression was dramatically reduced from Day 5 to Day 30. Surprisingly, the expression of Neurofilament (NF) is the intermediate filament which is found in the cytoplasm of a neuron was increased 2 fold at Day 5 [88]. Then expression was reduced on Day 10 but increased through Day 30 as indicated in Figure 3.5..

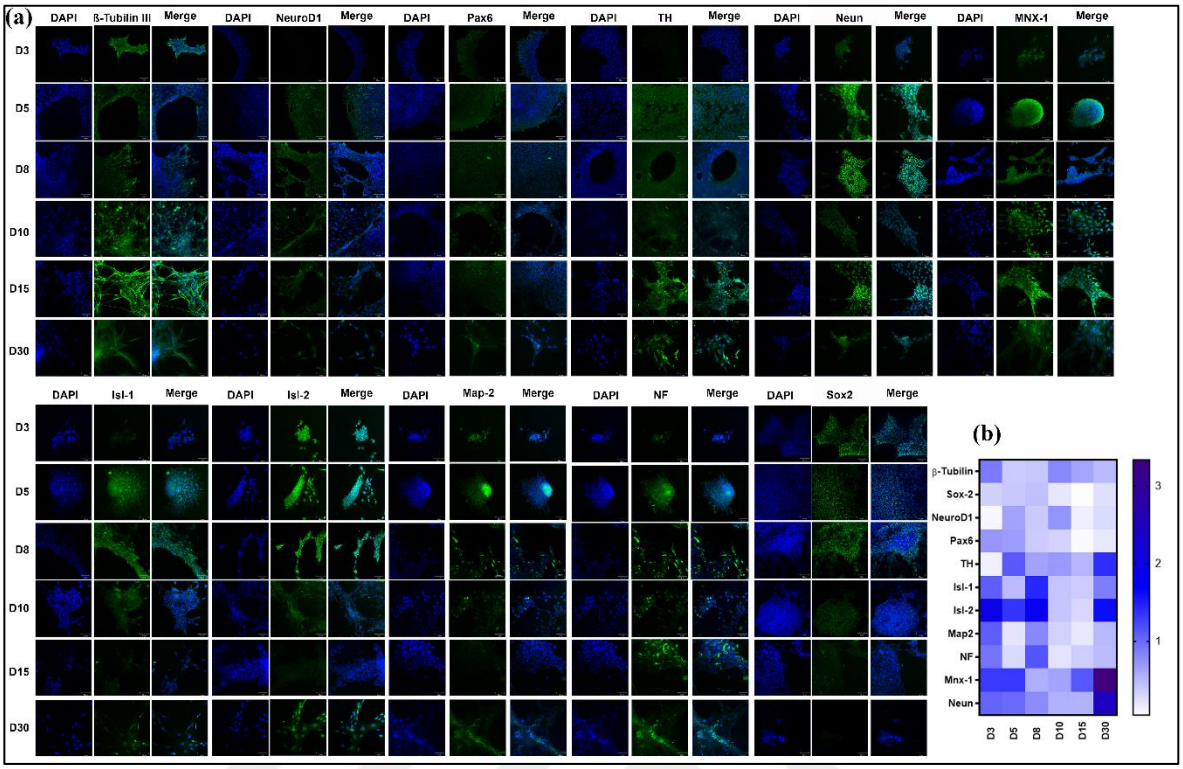

Figure 3.5. Immunocytochemical analysis of Neural markers. (a) Immunostaining of SC neurons at day 0, day 3, day 10, day 15 and day 30 was taken by confocal microscope at 20X magnification. (b) Heat map representation of expression levels of SC neurons

3.3.3 Flou-4 Staining and Live Cell Analysis

In live cell, Fluo-4 intensity of cells was measured for detection of calcium influx on Day 15, Day 30 and Day 40. At the one section of cells, it was demonstrated that increased and reduced Fluo-4 intensity according to time (Figure 3.6). The cells at Day 15, Day 30 and Day 40 Fluo-4 intensity was increased 1.2 fold, 1.4 fold and 1.5 fold, respectively. To compare day, SC neurons at Day 30 had more intensity than Day 15 and Day 40. Conversely, the Fluo-4 intensity of two cells was measured in a 10-second interval it was shown in Figure 3.3.4a. The peak of intensity was shifted according to 10-second period. It has been demonstrated that Fluo-4 intensity altered to depend on the distance as shown as Figure 3.7.. The fluo-4 intensity was decreased in a cell while it was increased in another cell.

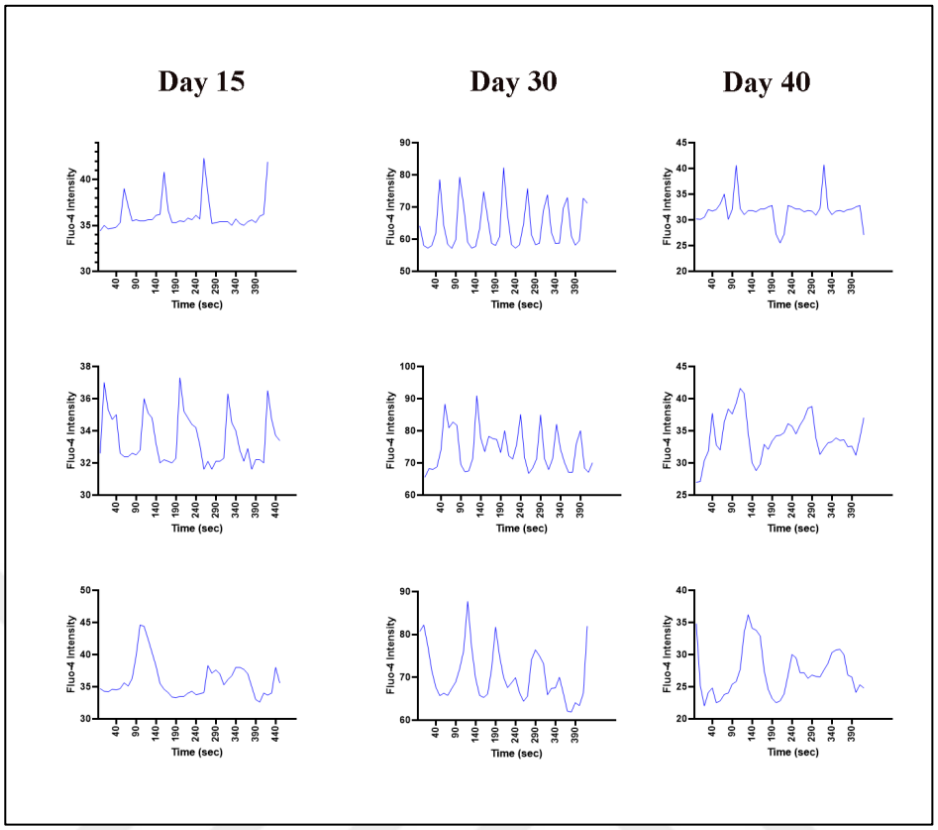

Figure 3.6. The graphs of Fluo-4 intensity versus time (seconds) of three different cells on Day 15, Day 30 and Day 40

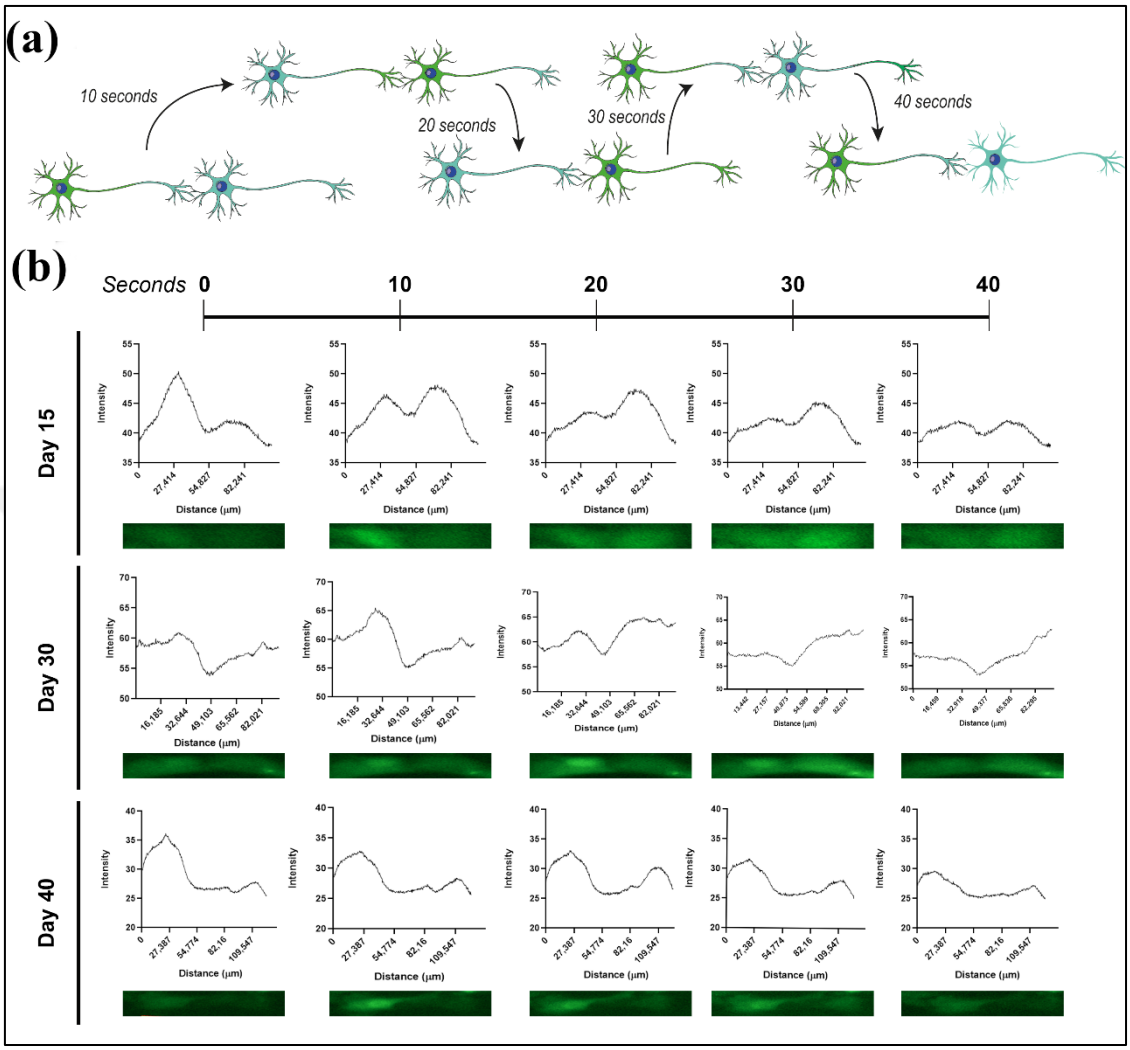

Figure 3.7. The graphs of Fluo-4 intensity versus distance according to 10-second intervals. (a) Schematic representation of Fluo-4 intensity measurement between two cells. (b) The graphs of intensity versus distance were indicated for 10 seconds intervals

3.3.4. Protein Profiling

The protein expression of cells obtained from day 0, day 3, day 10, day 15 and day 35 was detected by LC-MS analysis. According to LC-MS results, a heat map indicates that NMPs (Day 3) and spinal cord (SC) neurons at Day 10 were closest group with respect to protein expression levels and protein expression of SC neurons at Day 15 was close to SC neurons at Day 35. Additionally, the hierarchical cluster analysis demonstrated that Day 35 SC neurons and Day 15 neurons were close with 31.5 percent PCA (Figure 3.8a-b).

The proteins decreased and increased genes concerning Day 35 were detected and indicated profile plot as Figure 3.8c-e. The number of decreased proteins through Day 35 that indicated by blue line was 49 and number of increased proteins that indicated by red line was 44. Acetylcholine leads increasing mucus-secreting with free calcium ions in the cells and it binds to synaptotagmin that established by synaptobrevin, syntaxin and Synaptosomal-associated protein 23 (SNAP23) [89]. It causes membrane fusion and release vesicles. It has been found that the SNAP23 protein expression was increased through Day 35. Also, alpha centractin which is involving microtubule-based vesicle motility and is associated with centrosome [89] and Myosin regulatory light chain MRCL3 variant protein expression was increased through Day 35 as indicated Table 3.1..

The Venn diagram indicated the common and unique proteins of all days. The number of proteins that expressed all groups was 1589 (Figure 3.9a). 17 proteins were expressed commonly on Day 10, 15, and 35. The protein was only expressed on iPSCs (Day 0) was 13. Although there was no protein interaction on Day 0 cells in Figure 3.9b. To examine the molecular function and found in the tissue of expressed protein on Day 0, found in placenta as expected because iPSCs (D0) shows embryonic stem cells characteristics. Protein-protein interaction was obtained from common proteins on Day 10 Day 15 and Day 35 as indicated in Figure 3.9b-c. Day 0 cells have taken part in cellular component development and biogenesis (Figure 3.9f)

KRT14 is keratin 14, cytoskeletal protein that groups of intermediate filaments [90] and MACF1, microtubule actin crosslinking factor 1, is formed different bridges of microtubule [91]. RAB21 is the family GTPases, play role in cellular trafficking and can regulate migration and involved in neurite outgrowth. High expression of this gene is obtained from glioma patiemts [89]. These three-protein had protein-protein interactions as indicated in Figure 3.9c. MACF1 also interacted with SYNE2 (Spectrin Repeat Containing, Nuclear Envelope) which binds to F-actin and allows nucleus-centrosome attachment [89]. The proteins on Day 10, Day 15 and Day 35 have been found in the spinal cord, cerebellum, and brain. Fibrillin 2 and Keratinocyte-associated protein 2 were common proteins that were highly expressed at Day10, Day 15 and Day 35 SC neurons. Fibrillin 2 is a glycoprotein that plays role in perimysium and endomysium including muscle involvement [92]. Keratinocyte associated protein families are responsible for the regulation of neurite outgrowth and maintaining neuronal networks [93]. The molecular function of common proteins on Day 10, Day 15 and Day 35 were protein localization of the nucleus, axonal transport, embryonic skeletal cell development and gliogenesis that is the development of glial cells (Figure 3.9g).

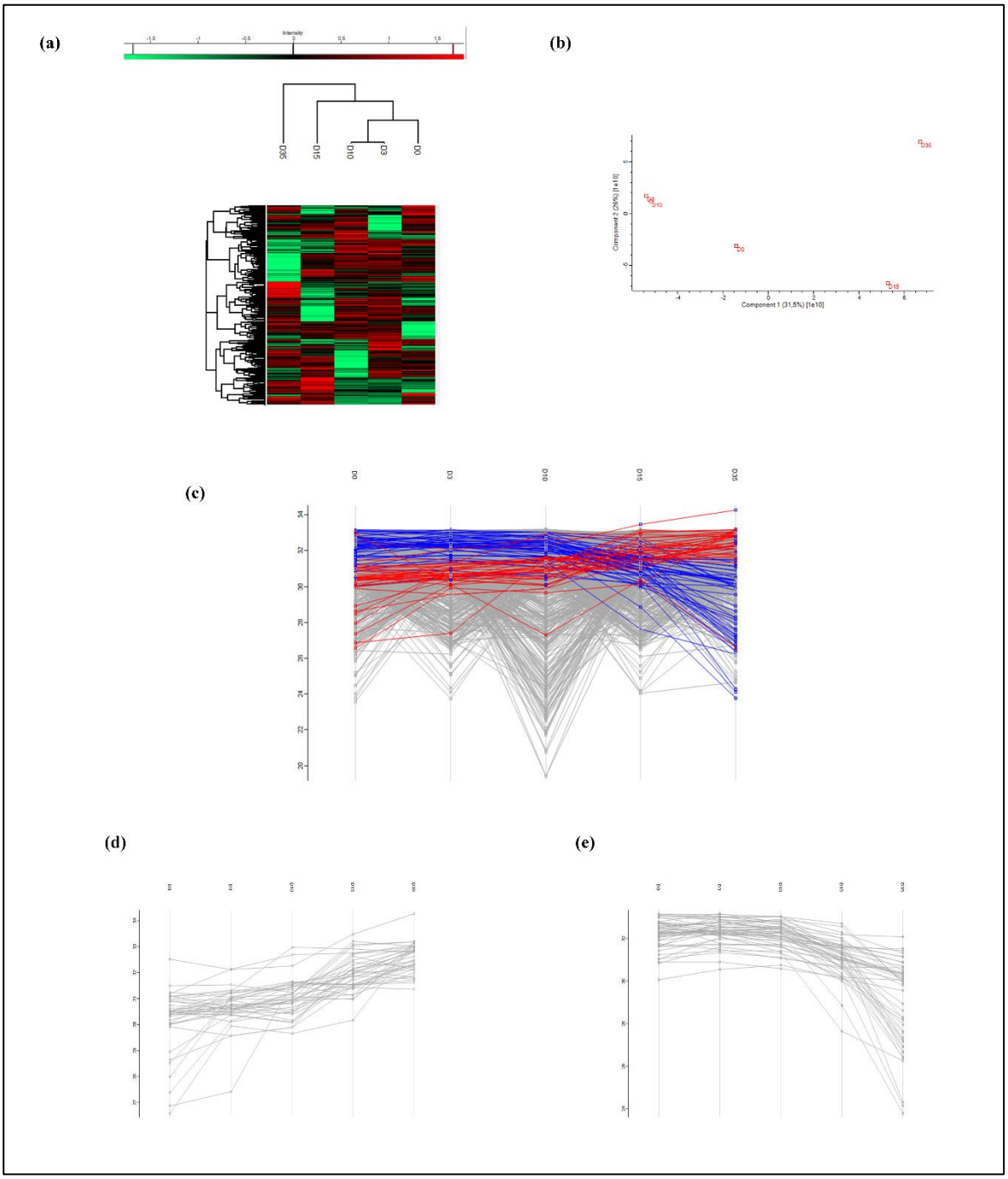

Figure 3.8. Protein profiling analysis of SC neurons at day 0, day 3, day 10, day 15 and day 35 (a) Heat map representation of protein profile at day 0, day 3, day 10, day 15 and day 35. (b) PCA analysis of protein profile. (c) Profile plot of proteins increasing (red) and decreasing (blue) through Day 35. (d) Profile plot of increased genes through Day 35. (e) Profile plot of proteins decreased through Day 35

Table 3.1. List of decreased and increased proteins from Day 0 to Day 35

Decreased Proteins	**Increased Proteins**
Adenosylhomocysteinase	Acetyltransferase component of pyruvate dehydrogenase complex
Cytoplasmic dynein 1 light intermediate chain 1	Ribosomal protein S5, isoform CRA_a
Coatomer subunit gamma-1	V-type proton ATPase subunit G
Translocon-associated protein subunit gamma	Importin subunit alpha
PAT complex subunit CCDC47	60S ribosomal protein L17
Retinol dehydrogenase 11	Replication protein A3, 14kDa
Procollagen galactosyltransferase 1	DNA-directed RNA polymerase II subunit RPB11-b1
Glutathione peroxidase	COP9 signalosome complex subunit 1
60S ribosomal protein L29	cDNA FLJ75365, highly similar to Homo sapiens SUGT1B (SUGT1) mRN
Histone HIST2H3PS2	60S ribosomal protein L23a
Isoleucyl-tRNA synthetase	SUMO-conjugating enzyme UBC9
Mitochondrial carrier homolog 2 variant	Alkaline phosphatase
Hsp90 chaperone protein kinase-targeting subunit	cDNA FLJ10442 fis, clone NT2RP1000738/Negative elongation factor A
Caprin-1	Serine/threonine-protein kinase 26
Acetyl-CoA carboxylase 1	LPP protein
Histone-binding protein RBBP4	Cytochrome c oxidase subunit 2
Serine/threonine-protein phosphatase PP1-alpha catalytic subunit	Synaptosomal-associated protein s23
Small ubiquitin-related modifier 2	Heterogeneous nuclear ribonucleoprotein Q
Eukaryotic initiation factor 4A-I	NADH-cytochrome b5 reductase 3

Eukaryotic translation initiation factor 3 subunit E	Dolichyl-diphosphooligosaccharide--protein glycosyltransferase subunit 1
Coatomer subunit alpha	Histidine--tRNA ligase, cytoplasmic
B-cell receptor-associated protein 31	ADP-ribosylation factor 4
40S ribosomal protein S27	Regulator of chromosome condensation
Glycine--tRNA ligase	MARCKS-related protein
Serine hydroxymethyltransferase, mitochondrial	Microfibrillar-associated protein 1
Transketolase	Alpha-centractin
Proteasome subunit alpha type-4	Actin, cytoplasmic 2
Elongation factor 2	A-kinase anchor protein 12
Eukaryotic translation initiation factor 2 subunit 1	Mannosyl-oligosaccharide glucosidase
Asparagine--tRNA ligase, cytoplasmic	Farnesyl pyrophosphate synthetase like-4 protein
26S proteasome non-ATPase regulatory subunit 14	ATP-citrate (pro-S-)-lyase
Proteasome subunit alpha type	Myosin regulatory light chain MRCL3 variant
Heterogeneous nuclear ribonucleoproteins C1/C2	RNA transcription, translation and transport factor protein
Lon protease homolog, mitochondrial	Putative histone H2B type 2-C
Eukaryotic translation initiation factor 3 subunit C-like protein	Histone-arginine methyltransferase CARM1
Eukaryotic translation initiation factor 3 subunit F	Acidic leucine-rich nuclear phosphoprotein 32 family member E
cDNA FLJ12434 fis, clone NT2RM1000037, highly similar to Homo sapiens KIAA0690 protein	Golgi resident protein GCP60
cDNA, FLJ96718, highly similar to Homo sapiens splicing factor, arginine/serine-rich 10	Serine/arginine repetitive matrix protein 2

(transformer 2 homolog, Drosophila) (SFRS10), mRNA	
Glucose-6-phosphate 1-dehydrogenase	Myosin regulatory light chain MRCL3 variant
T-complex protein 1 subunit delta	RNA transcription, translation and transport factor protein
p180/ribosome receptor	Putative histone H2B type 2-C
Serine/threonine-protein phosphatase 2A 56 kDa regulatory subunit	Histone-arginine methyltransferase CARM1
Dolichyl-diphosphooligosaccharide--protein glycosyltransferase 48 kDa subunit	Acidic leucine-rich nuclear phosphoprotein 32 family member E
60S ribosomal protein L38	Golgi resident protein GCP60
DNA replication licensing factor MCM4	
Methylsterol monooxygenase 1	
60S ribosomal protein L27	
Tyrosine 3-monooxygenase/tryptophan 5-monooxygenase activation protein, eta polypeptide, isoform CRA_b	

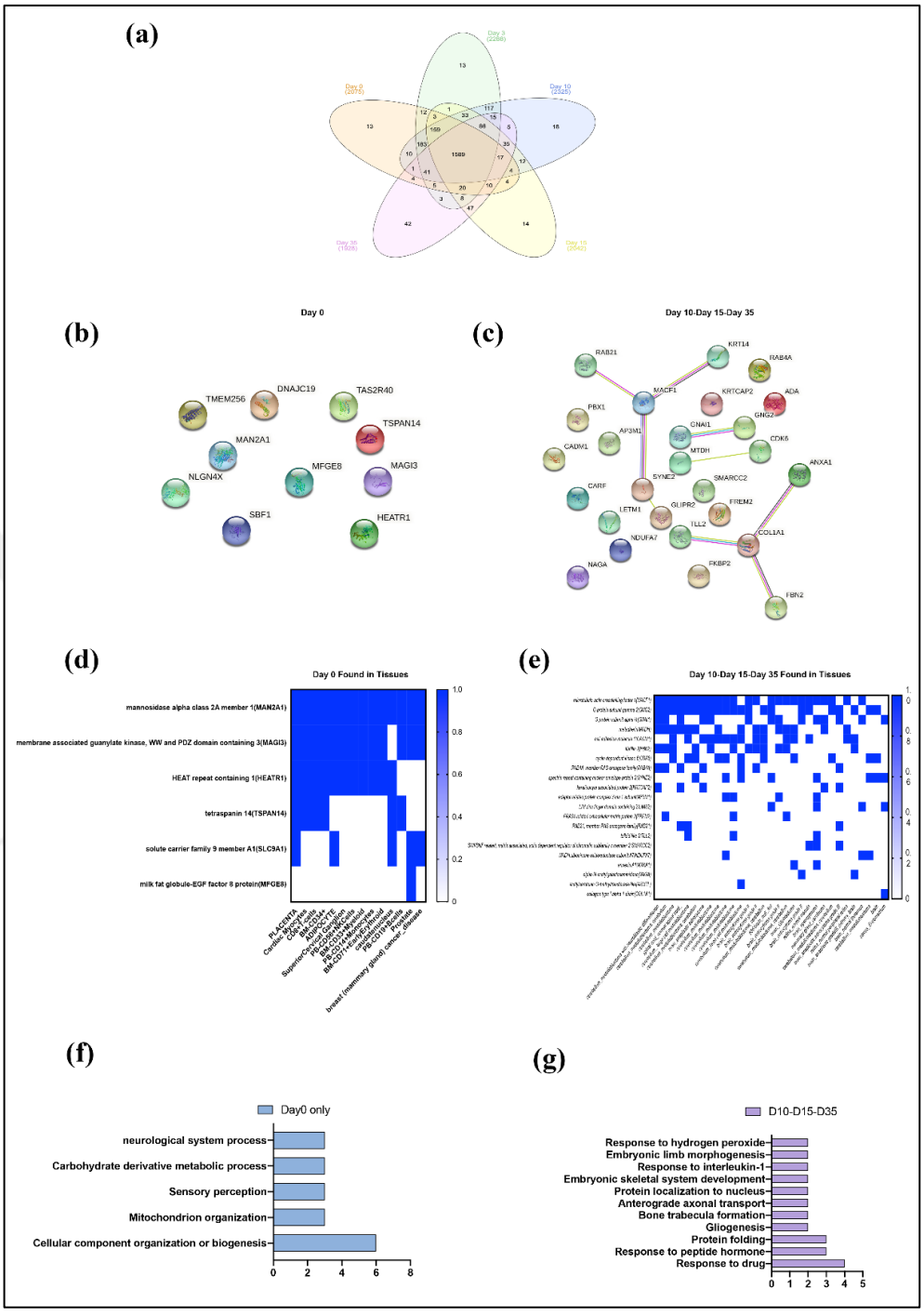

Figure 3.9. Protein profiling of common genes of SC neurons at Day 0, Day 3, Day 10, Day 15, Day 35 (a) Venn diagram of common proteins SC neurons at ay 0, Day 3, Day 10, Day 15, Day 35 (b) Protein-protein interactions of Day 0 cells (c) Protein-protein interactions of common protein of Day 10, Day 15 and Day 35. (d) The graphs of protein which found in tissue at Day 0. (e) The graphs of proteins which found in tissues at Day 10, 15, 35. (f) The genes related in biologic process at Day 0. (g) The common genes of Day 10, Day 15 and Day 35 related in biologic processand day

3.3.5. Gene Expression Level

The gene expression level of iPSCs (D0), NMPs (D3) and iPSCs derived SC neurons at Day 10, Day 23 and Day 35 was analysed by log starting quantity. The gene expression of Islet-1, MNX-1, Nkx6.2, and NeuroD1 were not changed significantly as shown in Figure 3.10.. On the other hand, Pax3 expression on iPSCs derived SC neurons was increased significantly to iPSCs. β-Tubulin expression was increased from NMPs to iPSCs derived SC neurons. Nkx1.2 and Nkx6.1 which are the transcription factor of neurogenesis were diminished significantly. Additionally, Hoxa4 which is expression increased on Day 10, Day 23 and Day 35 SC neurons with respect to iPSCs (D0). Neurog 2 is a transcription factor which play role in neurogenesis expression was also decreased on Day 35 SC neuron with respect iPSCs (D0).

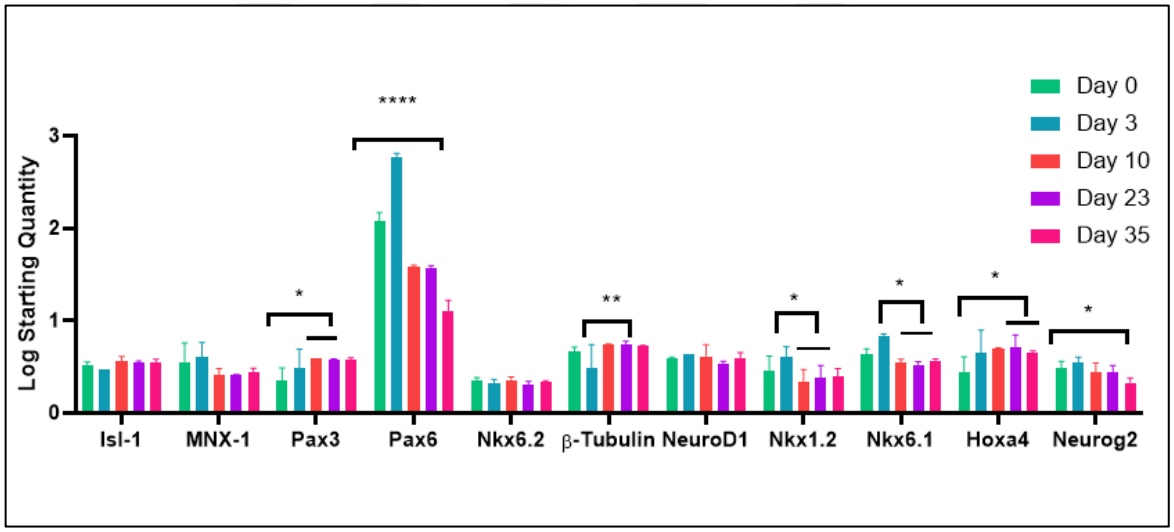

Figure 3.10. Gene expression level of iPSCs (D0), NMPs (D3), and iPSCs derived SC neurons at Day 10, Day 23 and Day 35. * p <0.05

3.4. NMP DERIVED SC NEURONS ESTABLISH NEUROMUSCULAR JUNCTION

3.4.1. Characterization of Myogenic Cells

Asc Telo cells were treated with a myogenic differentiation medium for 20 days in order to obtain myogenic cells. The differentiation protocol was indicated in Figure 3.11a and the medium contents were demonstrated at a Table in Figure 3.11b. Following the completion of the differentiation protocol, morphologic pictures of myogenic cells were taken by a light microscope. The extension of cells and muscle like structures were observed. In addition to morphologic pictures, myogenic marker expression was detected by ICC. MyoD and Desmin expression was determined in myogenic cells. On the other hand, MYH expression was obtained very slightly.

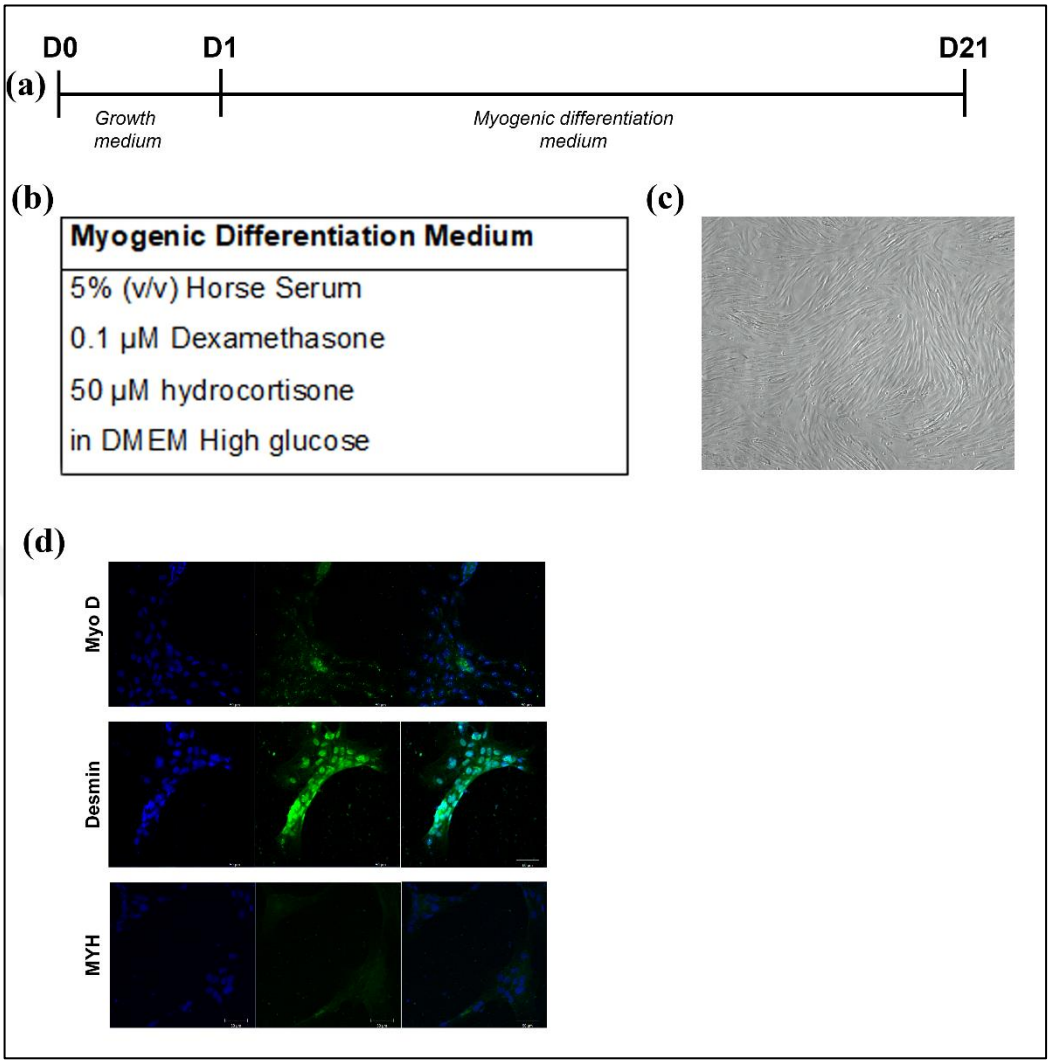

Figure 3.11. Characterization of myogenic cells. (a) Timeline of differentiation protocol of myogenic cells. (b) Differentiation medium contents of myogenic medium. (c) Morphologic pictures of myogenic cells. (d) Confocal microscope images of myogenic cells that were stained with MyoD, Desmin and MYH, Scale bar 50 µm

3.4.2. Co-culture of SC Neurons and Myogenic cells promote Neuromuscular Junction

Myogenic cells which were stained with PKH-26 labelled red and spinal cord neurons were co-cultured for a day and morphologic pictures were taken by live cells for 2 hours intervals. Both cells have not been competitive, the SC neurons were located on the myogenic cells. Besides, they were grown by a mutual and mimic neuromuscular junction. (Figure 3.12a) The calcium influx of co-cultured cells was examined by Fluo-4. At one point of cell, Fluo-4 intensity was remittent with respect to time as indicated in Figure 3.12b Fluo-4 intensity was measured between two cells for 10 minutes interval and demonstrated that Fluo-4 intensity has been increasing along to two cells. The signal was transduced to cell by cells. Although, the myogenic cells were seeded on insert migrated to SC neurons placed on the bottom of well, SC neurons were seeded on insert and were not migrated to myogenic cells placed on the bottom of the well as indicated in Figure 3.12.

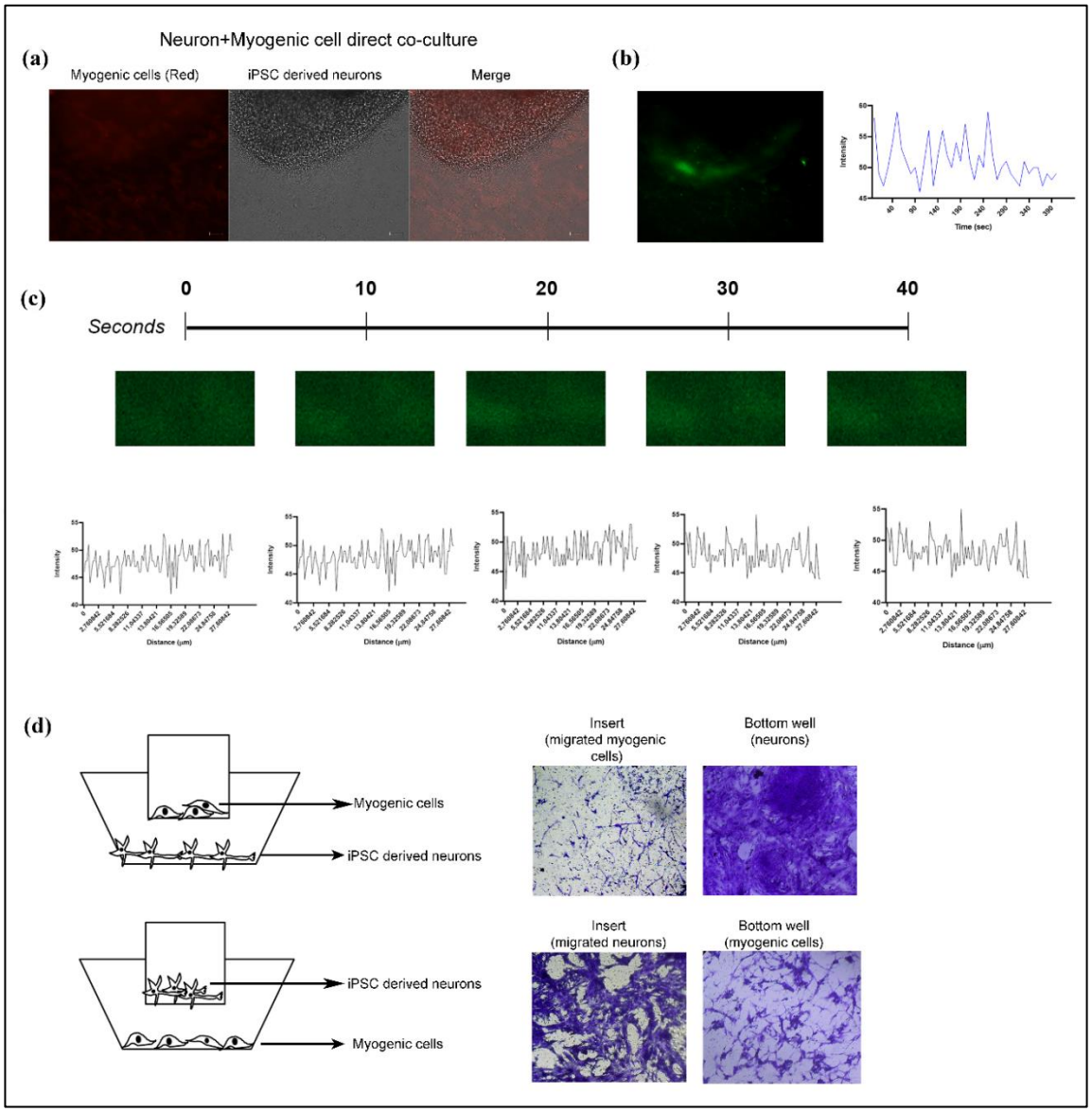

Figure 3.12. Neuromuscular junctions between SC neuron and myogenic cells (a) Live cell images of SC neurons and myogenic cells labelled red, Scale bar 50 μm. (b) Fluo-4 intensity of one point of cell. (c) Fluo-4 intensity graphs of between two cells. (d) Schematic representation of migration plate and microscope images of crystal violet-stained cells. Scale bar 200 μm

3.5. AXON ELONGATION

It has been shown that axon elongation and presence synaptic vesicles. As regards to this, SC neurons were transferred to Matrigel gelatine coated 10 cm dish and morphologic pictures were taken after a day to show attachment of cells and axon elongation pictures were taken at Day 2, Day 3 and Day 6. The process was demonstrated in Figure 3.13a. Axons of transferred SC neurons were attached after a day, and they were indicated in Figure 3.13b. SC neurons were placed with ganglions and axons were spreading at Day 0. At Day 2, 3 and 6, morphologic pictures of axons were taken, and branch analysis were done by Wimasis websites. The purple line was drawn by Wimasis which demonstrated to branch of axons in Figure 3.13c. According to the analysis of Wimasis, total branches were 1009, 588, 211 at Day 2, Day 3 and Day 6, respectively. In addition to this, circuity branch and branch points were decreased from Day 2 to Day 6. (Figure 3.13d). Moreover, under the light microscope, lipid particles were observed at the synapses of the neuron. The arrows indicated the spherical lipid particles in Figure 3.13e. According to this image, SC neurons were stained with Synaptophysin and phalloidin to stain F-actin. Synaptophysin expression was demonstrated at synapses of the neuron at 20X and 40X magnification and the arrow shows that spherical vesicles stained with synaptophysin. According to an analysis of TEM, synaptic vesicles were observed in Figure 3.13f. Additionally, SC neurons were visualized under SEM and axon structures were demonstrated and synaptic vesicles seem like white bubbles.

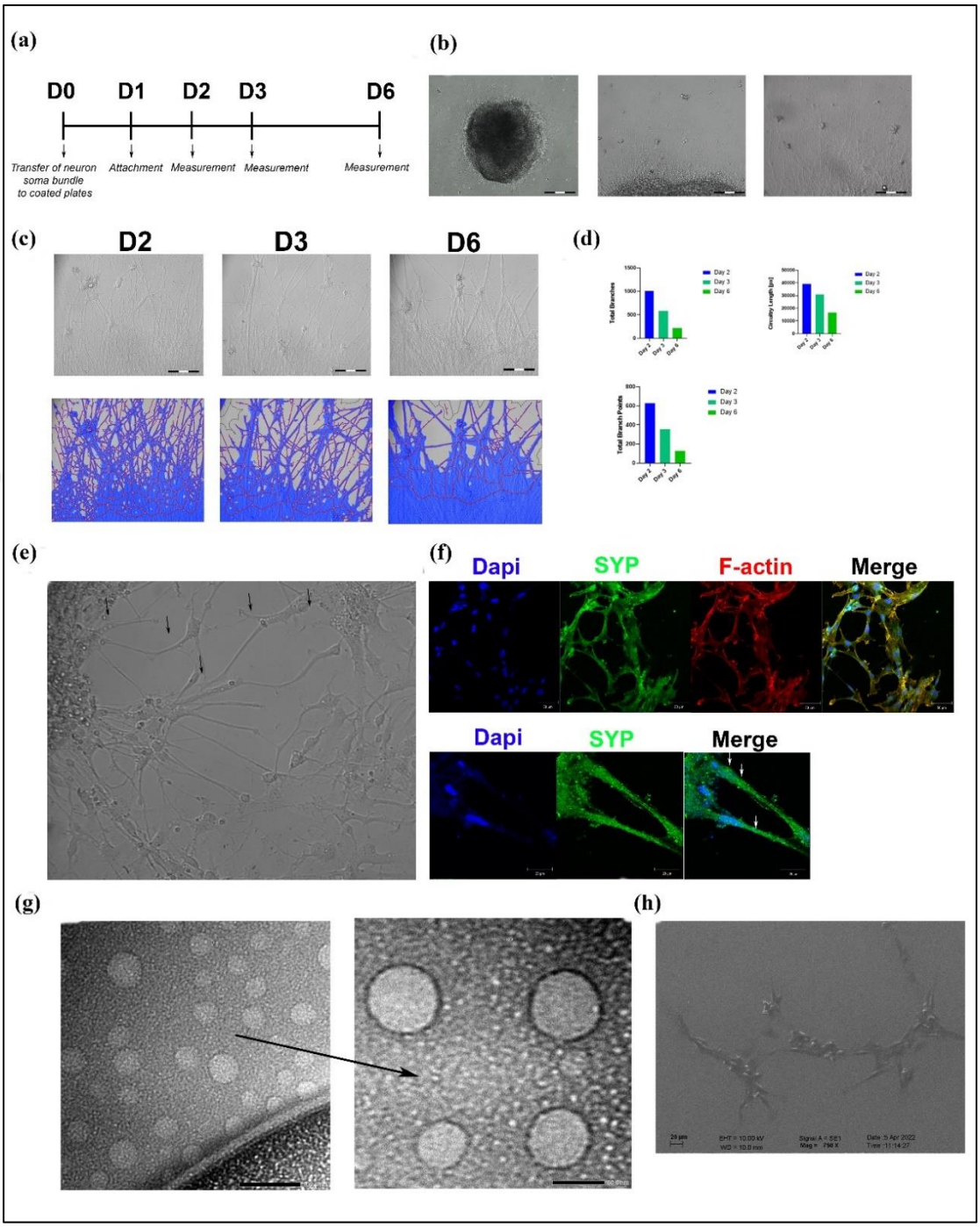

Figure 3.13. Axon Elongation analysis of SC neurons. (a) Timeline of axon elongation process. (b) Morphologic pictures of SC neurons were taken at Day 1. (c) Morphologic pictures and Wimasis analysis pictures of axons in SC neurons at Day 2, Day 3 and Day 6 (d) The graphs of circuity length, total branches and total branch points of axons that analyzed by Wimasis. (e) Synaptic vesicles were visualized by light microscope, Scale bar 200 µm (f) Immunostaining with Synaptophysin and Phalloidin on SC neurons, Scale bars 50µm, 20 µm, respectively. (g) TEM images of synaptic vesicles, Scale bar, 100nm, 50 nm, respectively. (h) SEM image of SC neurons, Scale bar 20 µm

3.6. CRYOPRESERVATION CAPACITY OF iPSCs DERIVED SPINAL CORD NEURONS

Mature spinal cord neurons at Day 30 were frozen and preserved for the short and long term. For short term cryopreservation, three different freezing solutions have been examined and short-term freezing neurons were thawed after a week, morphologic pictures were taken and freeze FBS containing media for three weeks as the timeline of cryopreservation indicated in Figure 3.14a. According to both short- and long-term cryopreservation, SC neurons have preserved morphologic structure (Figure 3.14b). SC neurons frozen with FBS containing media were seen healthy than other freezing media. However, it has not been observed proliferation of SC neurons which cryopreserved long term for 11 days (Figure 3.14c). Additionally, long term cryopreserved SC neurons also preserved calcium influx. The fluo-4 intensity was detected in long-term thawing neurons (Figure 3.14d)

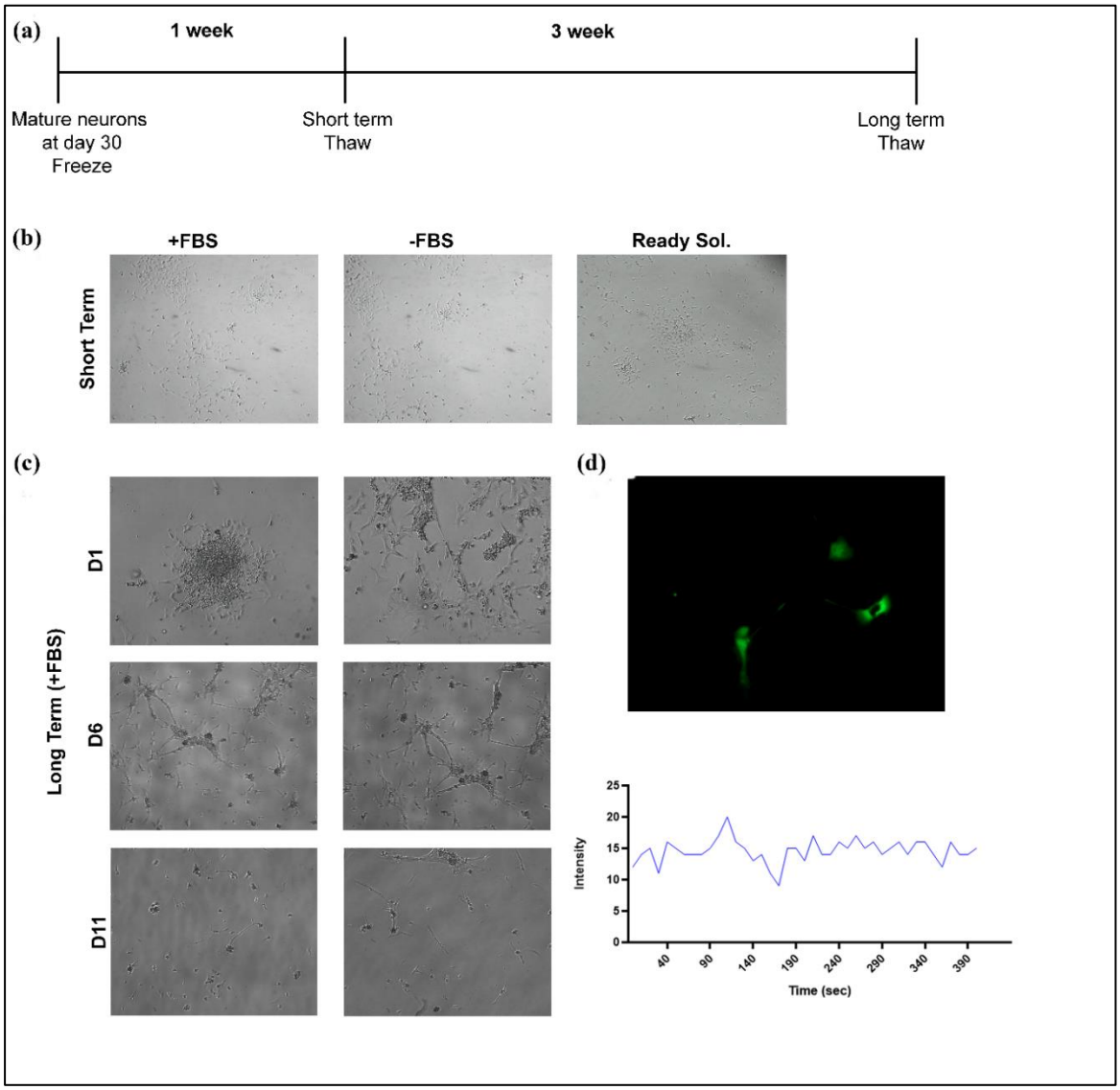

Figure 3.14. Cryopreservation capacity of SC neurons. (a) Timeline of cryopreservation protocol of SC neurons. (b) Morphologic pictures of short-term cryopreservation. Scale bar 200µm. (c) Morphologic pictures long-term cryopreservation of SC neurons on Day 1, Day 6 and Day 11. Scale bar 200µm. (d) Fluo-4 intensity pictures of long-term cryopreservation SC neurons and intensity versus time graph of Fluo-4

3. 7. MOUSE ES CELLS DIFFERENTIATE INTO SC NEURONS

mESCs were differentiated into spinal cord neurons for 30 days differentiation protocol. mESCs were supplied 12 ng per ml bFGF in N2B27 medium for 2 days. Then, 12 ng per ml bFGF and 3 μM CHIR In N2B27 medium and differentiate into NMP state. Following that, NMPs were differentiated to motor neurons with the 30 days differentiation protocol that is indicated in Figure 3.15.a. The morphological pictures were taken on Day 15 and Day 30. mESCs derived SC neuron had spindle-shaped and neuron-like structure was shown on Day 15. Additionally, axonal length and branch structure was demonstrated on Day 30 in Figure 3.15.b. Moreover, neuronal and progenitor markers expression weres examined by ICC on Day 15 and Day 30 mESCs derived neurons. Neural progenitor marker Pax6 and Isl-1 expression was reduced by 1.5-fold on Day 30 neurons and β-Tubulin III expression was increased by two-fold on Day 30 and MNX-1 expression was also increased on Day 30 (Figure3.15.c-d). On Day 30 mESCs derived SC neurons were examined for calcium influx by Fluo-4 for 15 minutes in a live cell. Accordingly, it was demonstrated that Fluo-4 intensity was increased and reduced according to time at a section of mESCs derived SC neuron (Figure 3.15.e). In addition, Fluo-4 intensity was measured for the 10-second interval and fluo-4 intensity of SC neurons was shifted according to the distance (Figure 3.15.f).

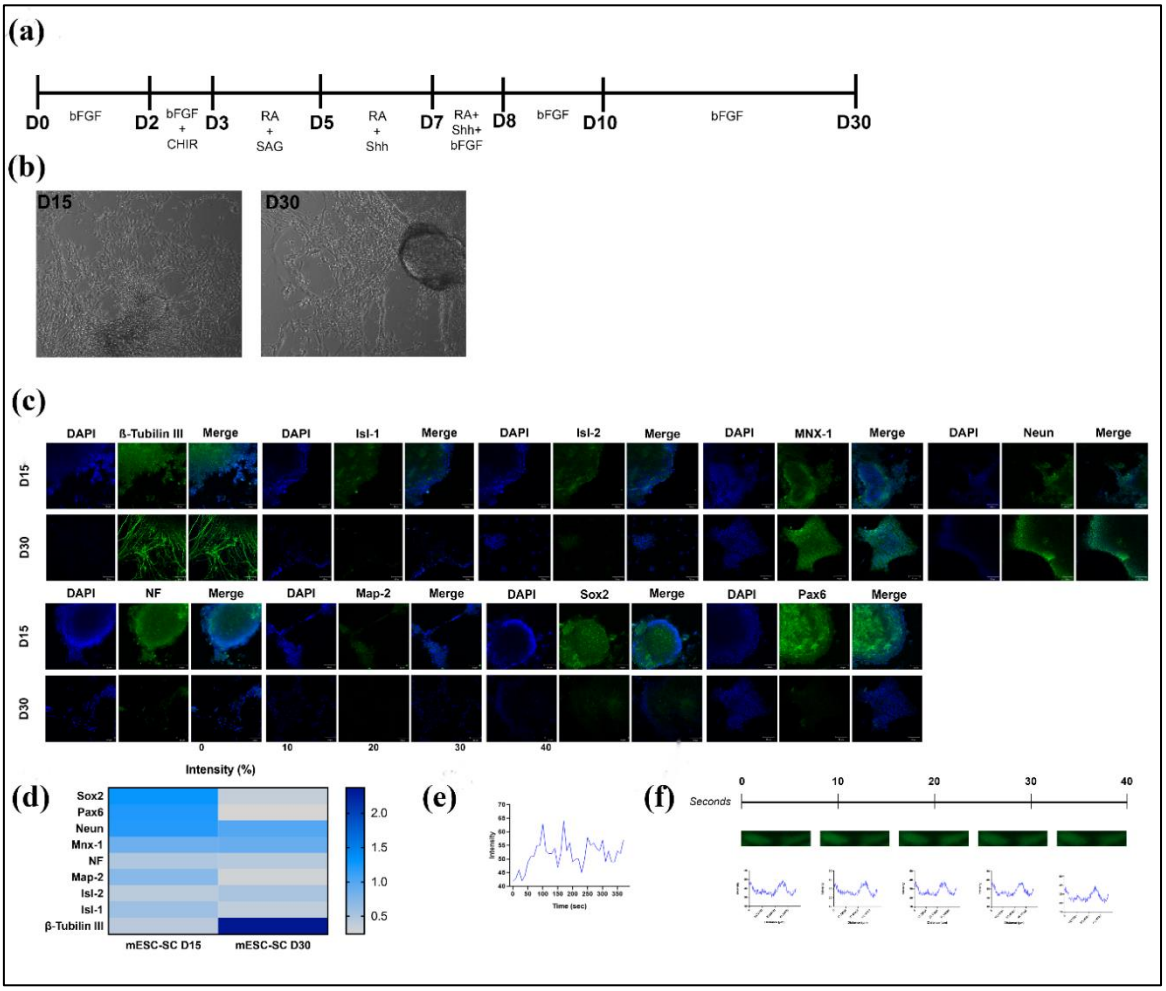

Figure 3.15. mESCs were differentiated into SC neurons. (a) Timeline of differentiation protocol. (b) Morphologic pictures of mESCs derived SC neurons at Day 15 and Day 30. Scale bar 200 μm. (c) Immunostaining of Day 15 and Day 30 mESC derived SC neurons. (d) Heat map of expression intensity of Day 15 and Day 30 mESCs derived SC neurons. (e) A line graph of Fluo-4 intensity differences with respect to time. (f) Fluo-4 intensity change according to distance

4. DISCUSSION

Motor neuron disease (MND) is a fatal, chronic, and progressive disease which occurs in destroying motor neurons. The motor neurons cannot control muscle cells in MND, which leads to problems in walking, breathing and speaking. Patients with MND lose control and activity of muscles. Amyotrophic lateral sclerosis (ALS) is the most common and fatal MND. The patients with ALS die within 2-5 years of diagnosis. The worldwide incidence of ALS is about 1- 3 per a hundred thousands people annually [94]. Men are at higher risk than women with a 1:2 ratio. Mean age of ALS onset is 51 between 66 years [95]. Although ALS arise in all ethnic and racial group worldwide, familial factor and oldest age are a more common risk factor of ALS [96]. 10 percent of ALS patients are familial ALS and 90 percent sporadic ALS. Smoking, heavy metals and playing football increase the risk of ALS [97] [98]. Furtherly, Spinal muscular atrophy (SMA) is another MND that is a fatal autosomal recessive disorder. SMA affects one in every 6,000 to one in every 10,000 live births, with a carrier frequency of 40 percent to 60 per.cent [99]. Moreover, Spinal cord injury (SCI) is the damage of neurons in the spinal cords. Vehicle accidents, falls, sports injuries and surgical complications result in SCI [101]. The epidemiology and demographic characteristics of spinal cord injury differ depending on location and period. In Turkey, an incidence of 8–21 cases per million people has been observed from various regions [100,101]

Cell-based therapy is targeting to provide new motor neuron that can allow to slow down or stop MND. The therapy will be promising to ALS or other MND. Early clinical trials have revealed that stem cells may be able to replace and repair damaged motor neurons in persons suffering from ALS/MND [100–104]. It has been demonstrated that 26 clinical trials of stem cell therapy completed about motor neuron diseases in the world. Half of them was Mesenchymal stem cell therapy, and 3 of them were hematopoietic stem cell therapy. Six of them are neural stem cells and only one was astrocytes derived from embryonic stem cells [105]. Bone marrow-derived mesenchymal stem cells (BM-MSC) -based therapy leads to slow the progression of motor neuron diseases [106]. Additionally, immunosuppression are not required because BM-MSCs are autologous [107].

Therefore, the identification of safe and effective cell therapy strategies is of interest for MND treatment. Development of efficient cellular differentiation protocols are required for pluripotent stem cell-based applications. The purpose of this thesis is to establish a protocol for functional motor neuron generation from human induced pluripotent stem cells via an intermediate NMP progenitor cell stage. In the current study, we aimed to generate an ex vivo protocol to obtain spinal cord motor neurons from their embryonic origin known as NMPs.

NMPs are bipotent progenitor cell populations that can generate to the spinal cord and paraxial mesoderm during embryonic development. NMPs are able to develop to posterior neural tissues that induce anterior neural plates [108,109]. The studies have indicated that mouse and human embryonic stem cells are directly NMPs and that the therapeutic use of NMPs can be increased [111]. According to the literature, NMPs are an important intermediate stage in the differentiation of mesoderm and mesenchymal stem cells from iPSCs [78]. Many motor neuron generation protocols aim to induce Hox genes, but this is insufficient. The protocol for NMP-derived motor neuron differentiation is promising for in vitro motor neuron generation [112,113]. iPSCs are reprogrammed stem cells which have the capacity to differentiate into all cell types in the body. Therefore, they are available cell therapy sources for important diseases such as neurodegenerative disorders. The most important advantage of using iPSCs for cell therapy is the ethical issues with embryonic cell cultivation because iPSCs are reprogrammed by somatic cells [114]. Additionally, iPSCs are also important for patient-specific therapy because they prevent allogeneic immune rejection [115]. Consequently, iPSCs are a convenient candidate for cell therapy. Since motor neurons cannot regenerate themselves, iPSCs are available as a source for motor neuron generation. Furthermore, iPSCs are obtained from different types of somatic cells such as blood cells [116], keratinocytes [117], melanocytes[118], adipogenic stem cells [119], and neural stem cell [120], and dermal fibroblast cells [121]. Yamanaka for the first time, created iPSCs from fibroblasts[29]. For this point, the generation of iPSCs from fibroblasts is the most common source. In this thesis, we generated iPSCs from human dermal fibroblast cells. Because dermal fibroblast cells have high reprogramming efficiency, and isolation procedures are easily. In addition, fibroblast cultivation and propagation are relatively easy and cost-effective [121].

According to literature, ALP activity, differentiation of three germ layers, expression of pluripotency marker and telomerase activity and chromosome abnormalities are the main characterization method of iPSCs [76,77,115]. In the current study, human iPSCs were generated HDFCs and they express pluripotent stem cell markers and have ALP activity. Three germ layer differentiation of iPSCs was tested by protein expression of Pax6, Sox17 and T/Bra.

In this study, the NMP population was characterized by co-expression of T/Bra and Sox2 at the gene and protein level. The results showed that iPSCs derived NMPs expressed hematopoietic mesodermal marker Mixl1 which requires differentiation of ventral mesoderm [112]. Wnt signalling play important role in the induction of mesoderm and the absence of Wnt signalling NMPs drive the spinal cord [123–125]. Wnt β-catenin signalling is required to drive mesodermal fate. Accordingly, it was examined Wnt3a expression and active β-catenin expression. Wnt3a expression was significantly increased with respect to iPSCs at day 0.

During the 40-day differentiation protocol, motor neuron and neuronal progenitor marker expression were detected by ICC and qPCR. While expression of neural progenitor markers was reduced with Sox2 and Pax6, motor neuron marker expression was increased with Mnx-1 and β-tubulin. Moreover, NMPs marker Sox2 expression was decreased with progressive differentiation protocol. Although β-tubulin expression was increased at both the protein and mRNA levels, MNX-1, a terminal motor neuron marker, was only increased at the protein level until Day 35. Pax 6 is the key transcription factor of neurogenesis [126]. Because Shh repressed Pax6 gene expression [127], gene and protein expression of Pax6 were reduced after 10 days of differentiation, as expected. According to the literature, progenitor cells are grouped into five ventral domains within the dorso-ventral axis of the neural tube [128]. It provides to give rise to interneuron and motor neurons. Furthermore, gene expression of Nkx6.1 and Nkx6.2 [50,129], which transcription factors have a role in differentiation to motor neuron progenitor domain, was also decreased as expected. Since NMPs can give rise to the spinal cord, they can be expressed as motor neuron progenitor marker Nkx6.1 (Figure 3.3.5) and highly expressed Pax6 as shown in Figure 3.5. and Figure 3.10..

The fact that neurons need more energy to transport synaptic vesicles and release neurotransmitters [130]. Therefore, the voltage-gated calcium channel help to an action potential to release neurotransmitters [131,132]. Calcium channels are important to pre-synaptic plasticity and deficiency of channels leads to neurological disorders [133]. For this reason, Fluo-4 intensity was measured iPSCs derived SC neurons to detect calcium influx in this study. Using live-cell imaging, SC neurons were visualized, and Fluo-4 intensity was measured for 30 minutes. The results demonstrated that iPSCs derived SC neurons had loaded calcium with respect to interval time, and calcium was passed in the cells. Accordingly, it had been examined the calcium transferring of the nearest two neurons mimics pre-synaptic and postsynaptic neurons. The calcium was transmitted from cell to cell. The study showed that iPSCs derived neurons transmit the impulse to another neuron at the following times. The results support that the iPSCs derived neurons had an action potential with voltage-gated calcium channels.

To characterize SC neurons, LC-MS analysis was performed and demonstrated protein profiling of iPSCs (D0) and NMPs (D3) and at Day 10, Day 15 and Day 35 iPSCs derived SC neurons. According to the analysis of protein profiling, iPSCs neurons on Day 15 and Day 35 were much closer than on other days. On the other hand, proteins of Day 10 iPSCs derived neurons show the similarity to NMPs (D3). These results indicate that after Day 10, iPSCs derived SC neurons have completed differentiation. To examine genes whose expression increased and decreased through Day 35, synaptic and tubulin related proteins such as KRT14 and MACF1 expression increased at Day 35. After 10 days of differentiation, when the common tissues found in SC neurons and the processes in which they were involved were examined, they were found in CNS. In addition, it has been found that genes that are common in each 3 days (D10, D15 and D35) were involved in axonal transport. The results support to iPSCs derived neuron after Day 15 have terminal state of motor neuron. Also, centrosome gene expression was increased until Day 35 (Table 3.3.4). Centrosome plays role in axon development and elongation [134]. Accordingly, elongation of axons was detected by transferring ganglion of SC neurons and taken pictures day by day. Using Wimasis website, branches of axons were measured and stated that branch point and branch number of axons were decreased with time and SC neurons tend to extend the length of axons. Besides, synaptic vesicles were visualized under the microscope according to Midorikawa et al 2015 [135]. In addition, synaptophysin is a calcium binding glycoprotein

that is found in presynaptic neurons [136], synaptophysin expression were seen at 40 X magnification through axon by spherical shapes. Finally, it was obtained lipid vesicles construction in TEM. Based on the literature, the study had visualized synaptic vesicles in TEM [137], the vesicles in Figure 3.5 can be synaptic vesicles. Therefore, we characterized synaptic vesicles using three different microscopy techniques.

Motor neurons can interact to muscle cells by neuromuscular junctions [138]. Accordingly, it was examined neuromuscular junction (NMJ) between iPSC derived neurons and myogenic cells. To mimic neuromuscular junction in vitro, it had been generated by myogenic cells. Myogenic cells are the muscle percussor cells that have ability to differentiate skeletal muscle cells [139]. The cells can express the myogenic marker of myogenin, myoD, Desmin and MYH [140]. In this thesis, myogenic cells were differentiated to mesenchymal stem cells of ASC Telo. Therefore, it was characterized by morphological and immunostaining with myoD, MYH and Desmin. These two cells could live together with not compete for each other. Neuromuscular junction assembled by pre-synaptic neuron and postsynaptic muscle fibers with neurotransmitter release. *in vitro* studies show the cocultured with muscle fibers and motor neurons formed NMJ [141]. According to this information, myogenic cells were cocultured with iPSCs derived SC neurons and measured Fluo-4 intensity. Results of the experiment indicate iPSCs derived SC neurons could live together with myogenic cells and transmitted to calcium.

Moreover, cryopreservation capacity was examined in order to the banking of cells. The previous studies about cryopreservation of neurons had been targeted to increase the efficiency of preservation [142,143]. Hence, both long- and short-term cryopreservation capacity was detected and FBS containing solution allowed high viability of SC neurons. Therefore, long term cryopreservation was done with FBS containing solution. After a month, SC neurons were thawed, and a few cells could live but they showed the same morphology. As a result, cryopreservation of SC neurons was not efficient, but it allows for the protection of neuron characteristics.

Finally, it has been examined that differentiation of mESCs into SC neurons using the same protocol. There was a difference in differentiation protocol that was the generation of NMPs. mESCs were obtained before human ESCs. Thus, mESCs were treated with bFGF containing media and then treated with CHIR [110]. End of the differentiation protocol, protein expression and calcium influx were examined. The results showed that mESCs derived neurons were also expressed MNX-1 and the presence calcium influx. To sum up, the protocol worked on mESCs differentiation. The results promising to allow *in vivo* experiments.

5. CONCLUSION

In conclusion, this thesis aimed to obtain fully functional spinal cord neurons from iPSCs via derivation of NMPs. The results of the thesis showed that iPSCs derived spinal cord neurons showed motor neuron characteristics for many aspects including gene expression, protein expression, synaptic vesicles construction, neuromuscular establishment and calcium influx. The protocol and generated neurons are successful ex vivo and needs to be tested in vivo for further projects. One of our future perspective and plan is to establish a spinal cord injury animal model prior to clinical trials. Our ultimate goal is to generate these neurons in GMP conditions for clinical trials. The results of this thesis and protocol might be used for therapeutic purposes in the near future.

REFERENCES

1. Blau HM, Brazelton TR, Weimann JM. The evolving concept of a stem cell: Entity or function? *Cell*. 2001;105(7):829–841.

2. Vats A, Tolley NS, Polak JM, Buttery LDK. Stem cells: sources and applications. *Clin Otolaryngol Allied Sci*. 2002;27(4):227–232.

3. Robey PG. Series Introduction: Stem cells near the century mark. *J Clin Invest.* 2000;105(11):89-91.

4. Moore KA, Lemischka IR. Stem cells and their niches. *Science.* 2006;311(5769):1880–1885.

5. Potten C. *Stem Cells.* Elsevier;1996.

6. Reubinoff BE, Pera MF, Fong CY, Trounson A, Bongso A. Embryonic stem cell lines from human blastocysts: somatic differentiation in vitro. *Nat Biotechnol.* 2000;18(4):399–404.

7. Howard D, Buttery LD, Shakesheff KM, Roberts SJ. Tissue engineering: strategies, stem cells and scaffolds. *Journal of Anatomy*. 2008;213(1):66-72.

8. Zakrzewski W, Dobrzyński M, Szymonowicz M, Rybak Z. Stem cells: past, present, and future. *Stem Cell Res Ther*. 2019;10(1):68.

9. Vacanti JP, Langer R. Tissue engineering: the design and fabrication of living replacement devices for surgical reconstruction and transplantation. *Lancet*. 1999;354:32–4.

10. Yamanaka S. A fresh look at iPS cells. *Cell*. 2009;137(1):13–7.

11. Biehl JK, Russell B. Introduction to Stem Cell Therapy. *J Cardiovasc Nurs*. 2009;24(2):98-103.

12. Augustin M. Preconditioning Methods in Cell Therapy of the Heart. Doctoral Thesis, University of Helsinki, 2012.

13. Wang P, McKnight KD, Wong DJ, Rodriguez RT, Sugiyama T, Gu X, et al. A Molecular Signature for Purified Definitive Endoderm Guides Differentiation and Isolation of Endoderm from Mouse and Human Embryonic Stem Cells. *Stem Cells Dev*. 2012;21(12):2273.

14. D'Amour, K., Agulnick, A., Eliazer, S. et al. Efficient differentiation of human embryonic stem cells to definitive endoderm. *Nat Biotechnol*. 2005;23:1534–1541.

15. Sasai Y, De Robertis EM. Ectodermal Patterning in Vertebrate Embryos. *Dev Biol*. 1997;182(1):5–20.

16. Alison MR, Poulsom R, Forbes S, Wright NA. Embryonic stem cells. *J Pathol*. 2002;197(4):424–9.

17. Wobus AM, Holzhausen H, Jäkel P, Schöneich J. Characterization of a pluripotent stem cell line derived from a mouse embryo. *Exp Cell Res*. 1984;152(1):212–9.

18. Conley BJ, Trounson AO, Mollard R. Human embryonic stem cells form embryoid bodies containing visceral endoderm-like derivatives. *Fetal Diagn Ther*. 2004;19(3):218–223.

19. Dayem AA, Lee S Bin, Kim K, Lim KM, Jeon T Il, Seok J, et al. Production of mesenchymal stem cells through stem cell reprogramming. *Int J Mol Sci*. 2019;20(8):1922.

20. Thomson JA, Itskovitz-Eldor J, Shapiro SS, et al. Embryonic stem cell lines derived from human blastocysts. *Science*. 1998;282(5391):1145-1147.

21. Richards M, Fong CY, Chan WK, Wong PC, Bongso A. Human feeders support prolonged undifferentiated growth of human inner cell masses and embryonic stem cells. *Nat Biotechnol*. 2002;20(9):933–6.

22. Yu J, Vodyanik MA, Smuga-Otto K, Antosiewicz-Bourget J, Frane JL, Tian S, et al. Induced pluripotent stem cell lines derived from human somatic cells. *Science*. 2007;318(5858):1917–1920.

23. Kerr CL, Hill CM, Blumenthal PD, Gearhart JD. Expression of pluripotent stem cell

markers in the human fetal ovary. *Hum Reprod*. 2008;23(3):589–599.

24. Doğan A. Embryonic Stem Cells in Development and Regenerative Medicine. *Adv Exp Med Biol*. 2018;1079:1–15.

25. Takahashi K, Yamanaka S. Induction of pluripotent stem cells from mouse embryonic and adult fibroblast cultures by defined factors. *Cell*. 2006;126(4):663–676.

26. Takahashi K, Tanabe K, Ohnuki M, Narita M, Ichisaka T, Tomoda K, et al. Induction of Pluripotent Stem Cells from Adult Human Fibroblasts by Defined Factors. *Cell*. 2007;131(5):861–872.

27. Chin MH, Mason MJ, Xie W, Volinia S, Singer M, Peterson C, et al. Induced Pluripotent Stem Cells and Embryonic Stem Cells Are Distinguished by Gene Expression Signatures. *Cell Stem Cell*. 2009;5(1):111–123.

28. Haas DL, Lutzko C, Logan AC, Cho GJ, Skelton D, Yu XJ, et al. The Moloney Murine Leukemia Virus Repressor Binding Site Represses Expression in Murine and Human Hematopoietic Stem Cells. *J Virol*. 2003;77(17):9439.

29. Ye L, Swingen C, Zhang J. Induced Pluripotent Stem Cells and Their Potential for Basic and Clinical Sciences. *Curr Cardiol Rev*. 2013;9(1):63.

30. Chambers I, Colby D, Robertson M, Nichols J, Lee S, Tweedie S, et al. Functional expression cloning of Nanog, a pluripotency sustaining factor in embryonic stem cells. *Cell*. 2003;113(5):643–655.

31. Yamanaka S. Induced Pluripotent Stem Cells: Past, Present, and Future. *Cell Stem Cell*. 2012;10(6):678–684.

32. Deng XY, Wang H, Wang T, Fang XT, Zou LL, Li ZY, et al. Non-viral methods for generating integration-free, induced pluripotent stem cells. *Curr Stem Cell Res Ther*. 2015;10(2):153–8.

33. Kriks S, Shim JW, Piao J, Ganat YM, Wakeman DR, Xie Z, et al. Dopamine neurons derived from human ES cells efficiently engraft in animal models of Parkinson's disease. *Nature*. 2011;480(7378):547–551.

34. Nori S, Okada Y, Yasuda A, Tsuji O, Takahashi Y, Kobayashi Y, et al. Grafted human-induced pluripotent stem-cell-derived neurospheres promote motor functional recovery after spinal cord injury in mice. *Proc Natl Acad Sci U S A*. 2 2011;108(40):16825-16830.

35. Liu H, Zhu F, Yong J, Zhang P, Hou P, Li H, et al. Generation of induced pluripotent stem cells from adult rhesus monkey fibroblasts. *Cell Stem Cell.* 2008;6:587–590.

36. West FD, Terlouw SL, Kwon DJ, Mumaw JL, Dhara SK, Hasneen K, et al. Porcine induced pluripotent stem cells produce chimeric offspring. *Stem Cells Dev*. 2010;19(8):1211–1220.

37. Shimada H, Nakada A, Hashimoto Y, Shigeno K, Shionoya Y, Nakamura T. Generation of canine induced pluripotent stem cells by retroviral transduction and chemical inhibitors. *Mol Reprod Dev*. 2010;77(1):2.

38. Wymeersch FJ, Huang Y, Blin G, Cambray N, Wilkie R, Wong FCK, et al. Position-dependent plasticity of distinct progenitor types in the primitive streak. *Elife*. 2016;5:e10042.

39. Cambray N, Wilson V. Two distinct sources for a population of maturing axial progenitors. *Development*. 2007;134(15):2829–2840.

40. Beddington RSP. An autoradio graphic analysis of tissue potency in different regions of the embryonic ectoderm during gastrulation in the mouse. *Embryol exp Morph*. 1982;69:265–285.

41. Tzouanacou E, Wegener A, Wymeersch FJ, Wilson V, Nicolas JF. Redefining the Progression of Lineage Segregations during Mammalian Embryogenesis by Clonal Analysis. *Dev Cell.* 2009;17(3):365–376.

42. Wilson PA, Hemmati-Brivanlou A. Induction of epidermis and inhibition of neural fate by Bmp-4. *Nature.* 1995;376(6538):331-333.

43. Sambasivan R, Steventon B, Martin BL. Neuromesodermal Progenitors : A Basis for Robust Axial Patterning in Development and Evolution. *Front. Cell Dev. Biol*. 2021;8(1):1–9.

44. Jankowska E. Spinal interneuronal systems: identification, multifunctional character and reconfigurations in mammals. *J Physiol*. 2001;533(1):31-40.

45. Stifani N. Motor neurons and the generation of spinal motor neuron diversity. *Front Cell Neurosci*. 2014;8:293.

46. Jessell TM. Neuronal specification in the spinal cord: inductive signals and transcriptional codes. *Nat Rev Genet*. 2000;1(1):20–9.

47. De Robertis EM. Spemann's organizer and self-regulation in amphibian embryos. *Nat Rev Mol Cell Biol*. 2006;7(4):296–302.

48. Stern CD. Neural induction: Old problem, new findings, yet more questions. *Development*. 2005;132(9):2007-2021.

49. Davis-dusenbery BN, Williams LA, Klim JR, Eggan K. How to make spinal motor neurons. *Development*. 2014;141(3):491–501.

50. Alaynick WA, Jessell TM, Pfaff SL. SnapShot: Spinal Cord Development. *Cell*. 2011;146(1):178-178.e1.

51. Dasen JS, Jessell TM. Hox networks and the origins of motor neuron diversity. *Curr Top Dev Biol*. 2009;88:169–200.

52. Philippidou P, Dasen JS. Hox genes: choreographers in neural development, architects of circuit organization. *Neuron*. 2013;80(1):12–34.

53. Pearson JC, Lemons D, McGinnis W. Modulating Hox gene functions during animal body patterning. *Nat Rev Genet*. 2005;6(12):893–904.

54. Tiryaki E, Horak HA. ALS and other motor neuron diseases. *Contin Lifelong Learn Neurol*. 2014;20(5):1185–1207.

55. Lunn JS, Sakowski SA, Federici T, Glass JD, Boulis NM, Feldman EL. Stem cell technology for the study and treatment of motor neuron diseases. *Regen Med*. 2011;6(2):201-213.

56. Kanning KC, Kaplan A, Henderson CE. Motor Neuron Diversity in Development and

Disease. *Annu Rev Neurosci.* 2010;33:409-440.

57. Straznicky C, Tay D. The localization of motoneuron pools innervating wing muscles in the chick. *Anat Embryol*. 1983;166(2):209–218.

58. Ravits JM, La Spada AR. ALS motor phenotype heterogeneity, focality, and spread. *Neurology*. 2009;73(10):805–811.

59. Trounson A. Embryonic stem cells. *Principles of Tissue Engineering*. 2007:421–429.

60. Orrell R, Orrell RW. Motor neuron disease: systematic reviews of treatment for ALS and SMA. *Br Med Bull*. 2010;93:145-159.

61. Ogino S, Leonard DGB, Rennert H, Ewens WJ, Wilson RB. Genetic risk assessment in carrier testing for spinal muscular atrophy. *Am J Med Genet.* 2002;110(4):301–307.

62. Pearn J. Classification of spinal muscular atrophies. *Lancet*. 1980;1(8174):919–922.

63. Lunn MR, Wang CH. Spinal muscular atrophy. *Lancet.* 2008;371: 2120–2133.

64. Kolb SJ, Kissel JT. Spinal Muscular Atrophy. *Neurol Clin.* 2015;33(4):831–846.

65. Lunn MR, Wang CH. Spinal muscular atrophy. *Lancet.* 2008;371(9630):2120–2133.

66. Markowitz JA, Tinkle MB, Fischbeck KH. Spinal muscular atrophy in the neonate. *J Obstet Gynecol neonatal Nurs*. 2004;33(1):12–20.

67. Nicolau S, Waldrop MA, Connolly AM, Mendell JR. Spinal Muscular Atrophy. *Semin Pediatr Neurol*. 2021;37:100878.

68. D'Amico A, Mercuri E, Tiziano FD, Bertini E. Spinal muscular atrophy. *Orphanet J Rare Dis.* 2011;6(1):1–10.

69. De Carvalho M, Matias T, Coelho F, Evangelista T, Pinto A, Sales Luís ML. Motor neuron disease presenting with respiratory failure. *J Neurol Sci.* 1996;139:117–122.

70. Mulder DW, Kurland LT, Offord KP, Beard M. Familial adult motor neuron disease: amyotrophic lateral sclerosis. *Neurology*. 1986;36(4):511–517.

71. Hedlund E, Hefferan MP, Marsala M, Isacson O. Cell therapy and stem cells in animal models of motor neuron disorders. *Eur J Neurosci*. 2007;26(7):1721–1737.

72. Karussis D, Karageorgiou C, Vaknin-Dembinsky A, Gowda-Kurkalli B, Gomori JM, Kassis I, et al. Safety and Immunological Effects of Mesenchymal Stem Cell Transplantation in Patients With Multiple Sclerosis and Amyotrophic Lateral Sclerosis. *Arch Neurol*. 2010;67(10):1187–1194.

73. Mazzini L, Mareschi K, Ferrero I, Miglioretti M, Stecco A, Servo S, et al. Mesenchymal stromal cell transplantation in amyotrophic lateral sclerosis: a long-term safety study. *Cytotherapy*. 2012;14(1):56–60.

74. Chen Y, Shao JZ, Xiang LX, Dong XJ, Zhang GR. Mesenchymal stem cells: A promising candidate in regenerative medicine. *Int J Biochem Cell Biol*. 2008;40(5):815–820.

75. Bredenkamp N, Yang J, Clarke J, Stirparo GG, von Meyenn F, Dietmann S, et al. Wnt Inhibition Facilitates RNA-Mediated Reprogramming of Human Somatic Cells to Naive Pluripotency. *Stem Cell Reports*. 2019;13(6):1083.

76. Martí M, Mulero L, Pardo C, Morera C, Carrió M, Laricchia-Robbio L, et al. Characterization of pluripotent stem cells. *Nat Protoc*. 2013;8(2):223–253.

77. Ward E, Twaroski K, Tolar J. Feeder-Free Derivation of Naive Human Pluripotent Stem Cells. *Stem Cells Dev*. 2017;26(15):1087–9.

78. Şenkal S, Hayal TB, Sağraç D, Şişli HB, Asutay AB, Kıratlı B, et al. Human ESC-derived Neuromesodermal Progenitors (NMPs) Successfully Differentiate into Mesenchymal Stem Cells (MSCs). *Stem Cell Rev Reports*. 2021;1:1–16.

79. Ruiz A, Alberdi E, Matute C. Mitochondrial Division Inhibitor 1 (mdivi-1) Protects Neurons against Excitotoxicity through the Modulation of Mitochondrial Function and Intracellular Ca 2+ Signaling. *Front Mol Neurosci.* 2018;11:3.

80. Akpinar G, Yoneten KK, Kasap M, Karaoz E. Search for Novel Plasma Membrane Proteins as Potential Biomarkers in Human Mesenchymal Stem Cells Derived from Dental Pulp, Adipose Tissue, Bone Marrow, and Hair Follicle. *J Membr Biol*.

2021;254(4):409–422.

81. Sherman BT, Hao M, Qiu J, Jiao X, Baseler MW, Lane HC, et al. DAVID: a web server for functional enrichment analysis and functional annotation of gene lists (2021 update). *Nucleic Acids Res*. *Nucleic Acids Res.* 2022;194.

82. Huang DW, Sherman BT, Lempicki RA. Systematic and integrative analysis of large gene lists using DAVID bioinformatics resources. *Nat Protoc*. 2009;4(1):44–57.

83. Heberle H, Meirelles VG, da Silva FR, Telles GP, Minghim R. InteractiVenn: A web-based tool for the analysis of sets through Venn diagrams. *BMC Bioinformatics.* 2015;16(1):1–7.

84. Dráberová E, Lukáš Z, Ivanyi D, Viklický V, Dráber P. Expression of class III β-tubulin in normal and neoplastic human tissues. *Histochem Cell Biol*. 1998;109(3):231–239.

85. Mullen RJ, Buck CR, Smith AM. NeuN, a neuronal specific nuclear protein in vertebrates. *Development*. 1992;116(1):201–211.

86. Kim KK, Adelstein RS, Kawamoto S. Identification of Neuronal Nuclei (NeuN) as Fox-3, a New Member of the Fox-1 Gene Family of Splicing Factors. *J Biol Chem*. 2009;284(45):31052–31061.

87. Danesin C, Agius E, Escalas N, Ai X, Emerson C, Cochard P, et al. Ventral neural progenitors switch toward an oligodendroglial fate in response to increased Sonic hedgehog (Shh) activity: Involvement of Sulfatase 1 in modulating Shh signaling in the ventral spinal cord. *J Neurosci*. 2006;26(19):5037–5048.

88. Hutchinson SA, Eisen J. Islet1 and Islet2 have equivalent abilities to promote motoneuron formation and to specify motoneuron subtype identity. *Development*. 2006;133(11):2137–2147.

89. Zucchi E, Bonetto V, Sorarù G, Martinelli I, Parchi P, Liguori R, et al. Neurofilaments in motor neuron disorders: towards promising diagnostic and prognostic biomarkers. *Mol Neurodegener*. 2020;15(1):1–20.

90. Lees-Miller JP, Helfman DM, Schroer TA. A vertebrate actin-related protein is a component of a multisubunit complex involved in microtubule-based vesicle motility. *Nature.* 1992;359(6392):244–246.

91. KRT14 keratin14 [Homo sapiens (human)]-Gene-NCBI; [cited 2022 Jun 29]. Availablefrom:https://www.ncbi.nlm.nih.gov/gene?Db=gene&Cmd=DetailsSearch &Term=3861.

92. MACF1 microtubule actin crosslinking factor 1 [Homo sapiens (human)]-Gene-NCBI; [cited 2022 Jun 29]. Available from: https://www.ncbi.nlm.nih.gov/gene?Db=gene&Cmd=DetailsSearch&Term=23499.

93. Holton JL, Ghiso J, Lashley T, Ganguly M, Strand K, Rostagno A, et al. Muscle fibrillin deficiency associated with Marfan's syndrome myopathy. *Neuropathol Appl Neurobiol.* 2002;28(2):155.

94. Yamada O, Tamura K, Yagihara H, Isotani M, Washizu T, Bonkobara M. Neuronal expression of keratinocyte-associated transmembrane protein-4, KCT-4, in mouse brain and its up-regulation by neurite outgrowth of Neuro-2a cells. *Neurosci Lett.* 2006;392(3):226–230.

95. Nelson LN. Epidemiology of ALS. *Clin Neurosci.* 1995;3(6):327–331.

96. van Es MA, Hardiman O, Chio A, Al-Chalabi A, Pasterkamp RJ, Veldink JH, et al. Amyotrophic lateral sclerosis. *Lancet*. 2017;390(10107):2084–2098.

97. Aboussouan LS, Khan SU, Meeker DP, Stelmach K, Mitsumoto H. Effect of noninvasive positive-pressure ventilation on survival in amyotrophic lateral sclerosis. *Ann Intern Med.* 1997;127(6):450–3.

98. Aktekin MR, Uysal H. Epidemiology of amyotrophic lateral sclerosis. *Turk Noroloji Derg*. 2020;26(3):187–196.

99. Al-Chalabi A, Hardiman O. The epidemiology of ALS: a conspiracy of genes, environment and time. *Nat Rev Neurol*. 2013;9:617–628.

100. Talbott EO, Malek AM, Lacomis D. The epidemiology of amyotrophic lateral

sclerosis. *Handb Clin Neurol.* 2016;138:225–238.

101. McDonald JW, Sadowsky C. Spinal-cord injury. *Lancet*. 2002;359(9304):417–425.

102. Karamehmetoğlu S, Ünal, Karacan I, Yilmaz H, Togay H, Ertekin M, et al. Traumatic spinal cord injuries in Istanbul, Turkey. An epidemiological study. *Paraplegia*. 1995;33(8):469-471.

103. Swinney MJ, Sepehri A, Stokic DS. Perception and predictors of health locus of control at rehabilitation discharge and 1 year after traumatic spinal cord injury. I*nt J Rehabil Res*. 2021;44(4):370–376.

104. Martínez HR, Molina-Lopez JF, González-Garza MT, Moreno-Cuevas JE, Caro-Osorio E, Gil-Valadez A, et al. Stem cell transplantation in amyotrophic lateral sclerosis patients: methodological approach, safety, and feasibility. *Cell Transplant*. 2012;21(9):1899–1907.

105. Mazzini L, Fagioli F, Boccaletti R, Mareschi K, Oliveri G, Olivieri C, et al. Stem cell therapy in amyotrophic lateral sclerosis: a methodological approach in humans. *Amyotroph Lateral Scler Other Motor Neuron Disord*. 2003;4(3):158–161.

106. Search of: stem cell therapy | Completed Studies | Motor Neuron Disease-List Results-ClinicalTrials.gov; [cited 2022 Jun 29]. Available from: https://clinicaltrials.gov/ct2/results?term=stem+cell+therapy&cond=Motor+Neuron+Disease&Search=Apply&recrs=e&age_v=&gndr=&type=&rslt=.

107. Aljabri A, Halawani A, Bin Lajdam G, Labban S, Alshehri S, Felemban R. The Safety and Efficacy of Stem Cell Therapy as an Emerging Therapy for ALS: A Systematic Review of Controlled Clinical Trials. *Front Neurol*. 2021;12:2125.

108. Woodbury D, Schwarz EJ, Prockop DJ, Black IB. Adult Rat and Human Bone Marrow Stromal Cells Differentiate Into Neurons. *J Neurosci Res*. 2000;61(4):364-370.

109. Tsakiridis A, Wilson V. Assessing the bipotency of in vitro-derived neuromesodermal progenitors. *F1000Res*. 2015;4:100.

110. Gouti M, Tsakiridis A, Wymeersch FJ, Huang Y, Kleinjung J, Wilson V, et al. In vitro generation of neuromesodermal progenitors reveals distinct roles for wnt signalling in the specification of spinal cord and paraxial mesoderm identity. *PLoS Biol.* 2014;12(8):e1001937.

111. Cooper F, Gentsch GE, Mitter R, Bouissou C, Healy L, Rodriguez AH, et al. Rostrocaudal patterning and neural crest differentiation of human pre-neural spinal cord progenitors in vitro. *Stem Cell Reports*. 2022;17(4):894-910.

112. Zhao J, Jiang WJ, Sun C, Hou CZ, Yang XM, Gao JG. Induced pluripotent stem cells: origins, applications, and future perspectives. *J Zhejiang Univ Sci B.* 2013;14(12):1059-1069.

113. Moradi S, Mahdizadeh H, Šarić T, Kim J, Harati J, Shahsavarani H, et al. Research and therapy with induced pluripotent stem cells (iPSCs): social, legal, and ethical considerations. *Stem Cell Res Ther*. 2019;10(1):1–13.

114. Raab S, Klingenstein M, Liebau S, Linta L. A Comparative View on Human Somatic Cell Sources for iPSC Generation. *Stem Cells Int.* 2014;2014:12.

115. Castro-Viñuelas R, Sanjurjo-Rodríguez C, Piñeiro-Ramil M, Hermida-Gómez T, Rodríguez-Fernández S, Oreiro N, et al. Generation and characterization of human induced pluripotent stem cells (iPSCs) from hand osteoarthritis patient-derived fibroblasts. *Sci Reports*. 2020;10(1):1–13.

116. Giorgetti A, Montserrat N, Aasen T, Gonzalez F, Rodríguez-Pizà I, Vassena R, et al. Generation of induced pluripotent stem cells from human cord blood using OCT4 and SOX2. *Cell Stem Cell*. 2009;5(4):353-357.

117. Sun N, Longaker MT, Wu JC. Human iPS Cell-Based Therapy: Considerations Before Clinical Applications. *Cell Cycle*. 2010;9(5):880-885.

118. Utikal J, Maherali N, Kulalert W, Hochedlinger K. Sox2 is dispensable for the reprogramming of melanocytes and melanoma cells into induced pluripotent stem cells. *J Cell Sci.* 2009;122(19):3502–3510.

119. Sun N, Panetta NJ, Gupta DM, Wilson KD, Lee A, Jia F, et al. Feeder-free derivation

of induced pluripotent stem cells from adult human adipose stem cells. *Proc Natl Acad Sci U S A.* 2009;106(37):15720–15725.

120. Kim JB, Greber B, Arazo-Bravo MJ, Meyer J, Park KI, Zaehres H, et al. Direct reprogramming of human neural stem cells by OCT4. *Nature.* 2009;461(7264):649–653.

121. Huangfu D, Osafune K, Maehr R, Guo W, Eijkelenboom A, Chen S, et al. Induction of pluripotent stem cells from primary human fibroblasts with only Oct4 and Sox2. *Nat Biotechnol*. 2008;26(11):1269–1275.

122. Ng ES, Azzola L, Sourris K, Robb L, Stanley EG, Elefanty AG. The primitive streak gene Mixl1 is required for efficient haematopoiesis and BMP4-induced ventral mesoderm patterning in differentiating ES cells. *Development.* 2005;132(5):873–884.

123. Henrique D, Abranches E, Verrier L, Storey KG. Neuromesodermal progenitors and the making of the spinal cord. *Development.* 2015;142(17):2864–2875.

124. Jones CC, Cook SF, Jarecki J, Belter L, Reyna SP, Staropoli J, et al. Spinal Muscular Atrophy (SMA) Subtype Concordance in Siblings: Findings From the Cure SMA Cohort. *J Neuromuscul Dis.* 2020;7(1):33–40.

125. Brahe C, Vitali T, Tiziano FD, Angelozzi C, Pinto AM, Borgo F, et al. Phenylbutyrate increases SMN gene expression in spinal muscular atrophy patients. *Eur J Hum Genet*. 2004;13(2):256–259.

126. Sansom SN, Griffiths DS, Faedo A, Kleinjan DJ, Ruan Y, Smith J, et al. The level of the transcription factor Pax6 is essential for controlling the balance between neural stem cell self-renewal and neurogenesis. *PLoS Genet.* 2009;5(6):e1000511.

127. Briscoe J, Pierani A, Jessell TM, Ericson J. A Homeodomain Protein Code Specifies Progenitor Cell Identity and Neuronal Fate in the Ventral Neural Tube. *Cell.* 2000;101(4):435–445.

128. Dasen JS, Jessell TM. Chapter Six Hox Networks and the Origins of Motor Neuron Diversity. *Curr Top Dev Biol*. 2009;88:169–200.

129. Sander M, Paydar S, Ericson J, Briscoe J, Berber E, German M, et al. Ventral neural patterning by Nkx homeobox genes: Nkx6.1 controls somatic motor neuron and ventral interneuron fates. *Genes Dev.* 2000;14(17):2134–2139.

130. Harris JJ, Jolivet R, Attwell D. Synaptic energy use and supply. *Neuron*. 2012;75(5):762–777.

131. Michael J Berridge. Neuronal Calcium Signaling Review. *Neuron*. 1998;21(1):13-26.

132. Clapham DE. Calcium Signaling. *Cell*. 2007;131(6):1047–1058.

133. Catterall WA, Few AP. Calcium Channel Regulation and Presynaptic Plasticity. *Neuron*. 2008;59(6):882–901.

134. Dotti CG, De Anda FC, Gärtner A. Control of Axon and Dendrite Identity and Structure. *Ref Modul Biomed Res.* 2014;2014.

135. Midorikawa M, Sakaba T. Imaging Exocytosis of Single Synaptic Vesicles at a Fast CNS Presynaptic Terminal. *Neuron*. 2015;88(3):492–498.

136. Wheeler TC, Chin LS, Li Y, Roudabush FL, Li A. Regulation of Synaptophysin Degradation by Mammalian Homologues of Seven in Absentia. *J Biol Chem*. 2002;277(12):10273–10282.

137. Steinkellner T, Madany M, Haberl MG, Zell V, Li C, Hu J, et al. A genetic probe for visualizing glutamatergic synapses and vesicles by 3D electron microscopy. A*CS Chem Neurosci*. 2021;12(4): 626–639.

138. Barbeau S, Tahraoui-Bories J, Legay C, Martinat C. Building neuromuscular junctions in vitro. *Development.* 2020;147(22):dev193920.

139. Hawke TJ, Garry DJ. Myogenic satellite cells: Physiology to molecular biology. *J Appl Physiol.* 2001;91(2):534–551.

140. Yu D, Cai Z, Li D, Zhang Y, He M, Yang Y, et al. Myogenic Differentiation of Stem Cells for Skeletal Muscle Regeneration. *Stem Cells Int.* 2021;2021:8884283.

141. Kaplan MM, Sultana N, Benedetti A, et al. Calcium Influx and Release Cooperatively

Regulate AChR Patterning and Motor Axon Outgrowth during Neuromuscular Junction Formation. *Cell Rep*. 2018;23(13):3891-3904.

142. Parker SS, Moutal A, Cai S, Chandrasekaran S, Roman MR, Koshy AA, et al. High Fidelity Cryopreservation and Recovery of Primary Rodent Cortical Neurons. *eNeuro*. 2018;5(5).

143. Drummond NJ, Singh Dolt K, Canham MA, Kilbride P, Morris GJ, Kunath T. Cryopreservation of Human Midbrain Dopaminergic Neural Progenitor Cells Poised for Neuronal Differentiation. *Front Cell Dev Biol.* 2020;8:578907.